Marine and Petroleum Geology 113 (2020) 104128

Contents lists available at ScienceDirect

Marine and Petroleum Geology

journal homepage: www.elsevier.com/locate/marpetgeo

Research paper

Filling characteristics, reservoir features and exploration significance of a volcanostratigraphic sequence in a half-graben basin —A case analysis of the Wangfu Rift Depression in Songliao Basin, NE China

Tang Huafeng[a,b,c,d], Zhao Xinying[e], Liu Xiang[f], Zhu Chenxi[a], Qu Weihua[f], Bian Weihua[a,*]

[a] College of Earth Sciences, Jilin University, Changchun, Jilin, 130061, China
[b] Department of Geological Sciences, University of Canterbury, Christchurch, 8140, New Zealand
[c] Key Laboratory for Evolution of Past Life and Environment in Northeast Asia (Jilin University), Ministry of Education, China
[d] Key Laboratory of Mineral Resources Evaluation in Northeast Asia,Ministry of Natural Resources, Changchun, 130061, China
[e] Shengli College China University of Petroleum, Dongying, Shandong 257061, China
[f] PetroChina Jilin Oil Field E&P Research Institute, Songyuan, Jilin 138000, China

A R T I C L E I N F O

Keywords:
Songliao Basin
Huoshiling Formation
Eruptive interval unconformity boundary
Volcanostratigraphy
Volcanic rocks
Reservoir origin

A B S T R A C T

It has long been considered that thicker volcanostratigraphic sequences should, in theory, contain more favourable reservoir conditions than in thinner sequences, particularly within large-scale stratovolcanoes found in sedimentary basins. However, drilling results from the Wangfu Rift Depression (WRD) in the Songliao Basin, China, show that the thick intermediate volcanostratigraphic sequence contains only one or two layers of favourable reservoir characteristics over approximately 1000 m of volcanic successions. The volcanostratigraphic sequence that is common in the graben basin has a particular distribution pattern as a result of reservoir and origin processes. The Eruptive Interval Unconformity Boundary (EIUB) is introduced and the burial history is investigated in order to determine the reservoir characteristics and origin. We also identify what controls the gas pool accumulation in the thick intermediate volcanostratigraphy. According to the reworked volcanic rocks and weathered crust patterns, the volcanostratigraphy of the basin has 13 wells containing one EIUB, and 2 wells with two EIUBs. The exposed and burial histories of the volcanostratigraphic sequence have produced a variety of pore space including primary pores, secondary pores and secondary fractures. The secondary pores are the most dominant, followed by primary pores and finally fractures. These pore spaces form a reservoir with moderate to low porosity and permeability and the most productive reservoirs are located 40–80 m below the EIUB. The secondary pores are primarily controlled by weathering and leaching as well as deep-burial alteration. Due to the migration of fluids from the overlying strata into the volcanic rocks of the Huoshiling Formation below, the top most layer dissolves first, which significantly enhances the secondary porosity of this layer found 40–80 m below the EIUB. Thus, the number of EIUBs should control the number of favourable reservoir layers. Based on analysis of the reservoir, source and cap rocks in the study area, we conclude that the best exploration targets in these thick volcanostratigraphic sequences, specifically in half-graben basins, are the volcanic inherited-uplift slope areas, followed by the inherited-uplift of the sag area and the uplifted zones. The findings presented in this work provide an insight of the evolution of porosity in other volcanic systems elsewhere and contribute to the likelihood of locating the favourable exploration targets for thick volcanostratigraphic sequences in half-graben basins.

1. Introduction

Volcanostratigrapy is an important aspect of all basins, as volcanic rocks can comprise up to 25% by volume of a basin (Einsele, 2000; Allen and Allen, 2013). Volcanic rock reservoirs are becoming an important new field in global oil and gas exploration because these reservoirs are widely distributed, found in more than 300 basins or blocks, in 20 countries, across 5 continents (Schutter, 2003). In recent years, prolific oil and gas reservoirs have been found in multiple basins in China; the Songliao Basin, Junggar Basin, Tarim Basin, and Liaohe Basin (Chen et al., 1999, 2016, 2017a, 2017b; Feng, 2008; Liu et al., 2010; Tang et al., 2012a). The volcanosedimentary sequence of the

* Corresponding author.
E-mail address: WeihuaBian@jlu.edu.cn (B. Weihua).

https://doi.org/10.1016/j.marpetgeo.2019.104128
Received 2 March 2019; Received in revised form 5 November 2019; Accepted 6 November 2019
Available online 09 November 2019
0264-8172/

basin may contribute to the potential oil and gas reservoirs and traps as well as assist in migration and accumulation of hydrocarbons (Stagpoole and Funnell, 2001; Polyansky et al., 2003; Jin et al., 2007; Filho et al., 2008; Tao et al., 2017; Tang et al., 2017a).

The volcanostratigraphic characteristics, reservoir-forming pattern and formation mechanism are important components of a volcanic reservoir study (Uliana et al., 1989; Antonio et al., 2012). Research in recent years has shown that the reservoir distribution is constrained by the volcanic edifice type and facies belts. For example, excellent reservoirs are often located in the central facies belts of composite volcanic edifices (Tang et al., 2008, 2012c; Wang and Chen, 2015; Yang et al., 2017). In central facies belts, productive reservoirs are particularly common in the upper part of lava flows, pyroclastic flows, in the volcanic neck and the inner part of the perlitic dome (Wang et al., 2006). The reservoir distribution characteristics are also constrained by the volcanostratigraphic textures, i.e., stratified, pseudostratified and massive textures (Mc Phie et al., 1993; Tang et al., 2011, 2012c; Yi et al., 2014). Thus, the identification of volcanostratigraphic characteristics can be used to determine the distribution pattern of a volcanic reservoir.

In theory, thicker volcanostratigraphic sequences should contain more layers with favourable reservoir characteristics, particularly in stratovolcanoes that were earlier discovered in the basins of China (Feng, 2008; Zou et al., 2011; Wang and Chen, 2015; Tang et al., 2018). However, drilling results show that thick intermediate volcanostratigrapy of the Wangfu Rift Depression (WRD) in the Songliao Basin has very few layers of favourable reservoir across 1000 m of volcanic successions. The origin and characteristics of these thick volcanic rock reservoirs is still poorly understood and the mechanisms behind the accumulation of gas pools found within will be of great importance in guiding further gas exploration in the basin.

The primary porosity of the volcanostratigrapy is related to the facies architecture (Cao et al., 1999; Kawamoto, 2001; Gu et al., 2002; Wu et al., 2006; Jerram et al., 2009; Tang et al., 2013, 2015; Watton et al., 2014; Chen et al., 2014a,b; Yi et al., 2016; Zheng et al., 2018). The secondary porosity is related to weathering and alteration processes as well as tectonic activities in the wider region (Luo et al., 1999; Kontorovich and Khomenko, 2001; Othman et al., 2002; Volk et al., 2002; Kus et al., 2005; Jones et al., 2007; Sruoga and Rubinstein, 2007; Feng et al., 2008; Wang et al., 2011; Huang et al., 2012; Hou et al., 2012). Furthermore, the porosity is constrained by the eruptive and buried history of the volcanics. The eruptive history of the buried volcanoes can be reconstructed according to the Eruptive Interval Unconformity Boundary (EIUB) (Tang et al., 2015; Yi et al., 2015). Here, the EIUB and burial history of volcanostratigraphic sequences in the Wangfu Rift Depression are introduced to determine the reservoir characteristics and origin, as well as to help to identify the controlling factor of gas pools in the thick intermediate volcanostratigraphy of the Songliao Basin. The main objectives of this study are to identify the characteristics and origin of the reservoir and the relation to the EIUB, and to analyse the favourable exploration targets in these thick volcanostratigraphic sequences found in half-graben basins.

2. Geological setting

The tectonic evolution of the Mesozoic-Cenozoic Songliao Basin of NE China can roughly be divided into three tectonic stages; a rifting phase with deposition of a syn-rift volcanogenic succession, a sagging stage forming a post-rift sedimentary sequence and a depauperization period consisting of a structurally inverted coarsening-upward sequence (Wang and Chen, 2015; Wang et al., 2016) (Fig. 1). Approximately 45 rift depressions were formed during the rift stage, including the WRD which covers an area of more than 2500 km^2 in the middle of the Songliao Basin (Fig. 2). Overlying the Palaeozoic metamorphic basement is an infilling sequence composed of Jurassic-Cretaceous rift-related volcanic and sedimentary rocks. The volcanic rocks are found widespread throughout the region in other rift depressions, and together, form a large igneous province (Jia et al., 2007; Cai et al., 2012) extending over an estimated area of 0.85×10^6 km^2 (0.328×10^6 mi^2). The volcanic activity of Huoshiling Formation, which lasted for 13 Myr (158–145 Ma) during the Jurassic (Wang et al., 1995, 2002), showed an eastward migration, reflecting tectonic changes during the different stages of collision between the Eurasian and Siberian plates. The emplacement of this huge volcanic unit is coeval with a regional lithospheric extensional regime that has been active since the Jurassic (Yang et al., 2005). The rift system is composed of oppositely oriented grabens that are controlled by NE-SW trending major faults (Ge et al., 2012). The WRD is terminated in the west by a NW to N-S strike fault and overlapped in the east. The eastern uplift area was inverted in late Tithonian to late Aptian, leading to the uplift and denudation of the Huoshiling Formation (Figs. 2b and 3). The WRD contains the Huoshiling, Shahezi and Yingcheng Formations (Jiang et al., 2017). The Huoshiling Formation can be divided into two members in the region. The first is dominated by sandy conglomerates, and the second by intermediate and basic volcanic rocks, mudstones and reworked volcanic deposits (Fig. 1). However, the first member of the formation is not found in boreholes in the WRD. The Shahezi Formation is dominated by mudstones and sandstones, and can also be divided into two members. The first member is comprised mainly of thick mudstone, while the second member is mainly sandstone. Finally, the Yingcheng Formation of the WRD is dominated by a combination of mudstone and sandstone, meaning it differs from the other rift depressions (Figs. 1 and 3).

3. Methods

The seismic data, well logs, and drill core data were obtained during the exploration of the WRD. Volcanic rocks (including reworked volcanic rocks) were identified in 15 wells by using 40 m cores, 1200 cutting samples, 6000 m of Fullbore Formation Mocroimager (FMI) data and Gamma Ray (GR) logging. The volcanostratigraphic filling characteristics were analysed by using an integrated method involving well logging and seismic data. The void spaces were assessed through a combination of macroscopic and thin section observations of resin-impregnated samples from cores. The exploration potential was assessed by using a combination of techniques involving the cores, well logging, seismic data and gas testing results.

Whole-rock analyses were performed on four fresh, unaltered volcanic rock samples. Major element compositions were determined by X-Ray Fluorescence (XRF) using a D/MAX-2400 instrument (manufactured by Rigaku Co, Ltd), in the Rock-Mineral Preparation and Analysis Lab at the Geology and Geophysics Research Institute of the Chinese Academy of Sciences, Beijing, China. Ferroporphyrin and ignition loss were measured by volumetric and gravimetric methods, respectively.

Porosity and permeability tests were conducted using the AP608 instrument at the Jilin University Rock Physics Lab (Changchun City, Jilin Province, China) through helium (He) injection. The test temperature was 22 °C, and testing was performed according to the standard method of the Petroleum Industry of the People's Republic of China (SY/T 5336-2006, “Cores Analytical Method”).

Capillary pressure measurements were carried out using the mercury intrusion method at the Fluid Mechanics Laboratory at the Daqing Oilfield Company E&D Research Institute using an AutoPore IV 9505 porosity analyser. The test temperature was 19.1 °C and humidity was 39% RH. The test followed the standard method of the Petroleum Industry of the People's Republic of China (SY/T 5346-2005: “Capillary Pressure Curve Measurements of Rocks”).

X-ray were conducted on 11 fresh samples. The samples were crushed and any visibly dirty rock debris was discarded. The test was performed at the Mineral and Petroleum Laboratory of the Department of Geology, Jilin University, using a RIGAKU D/MAX 2550/PC (Japan) instrument and the test standard SY/T5163-1995 “The X-ray diffraction

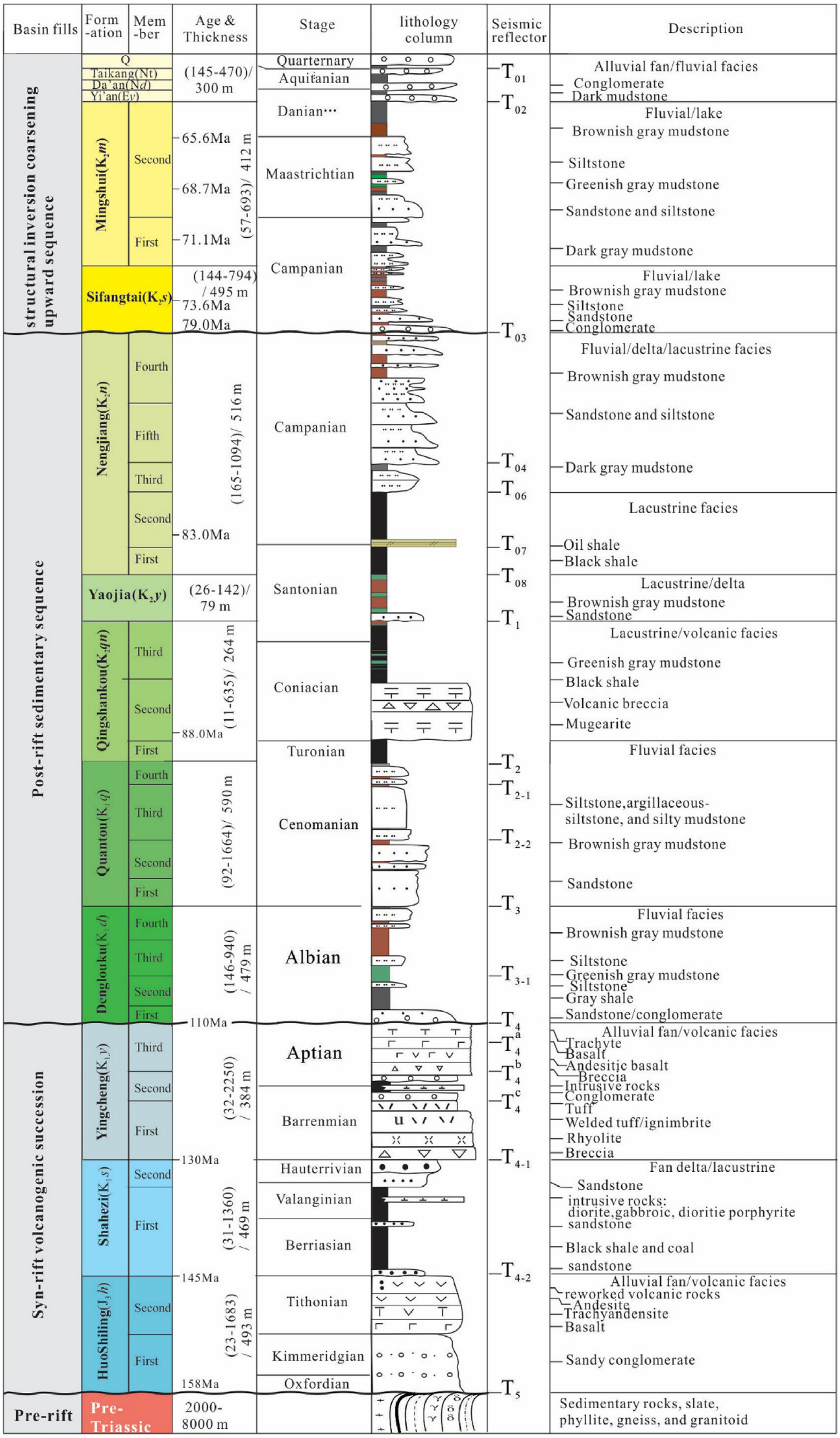

Fig. 1. Upper Mesozoic stratigraphic column for the Songliao Basin, showing three cycles of basin fill, (1) synrift, (2) super-rift, and (3) structural inversion. The volcanic reservoirs of Yangfu rift depression is in the upper Jurassic Huoshiling Formation (J_3h). Vertical numbers such as (32–2250)/384 m in the fourth column indicate borehole statistical data on formation thickness: (minimum-maximum)/mean. (After Wang and Chen, 2015; Wang et al., 2016).

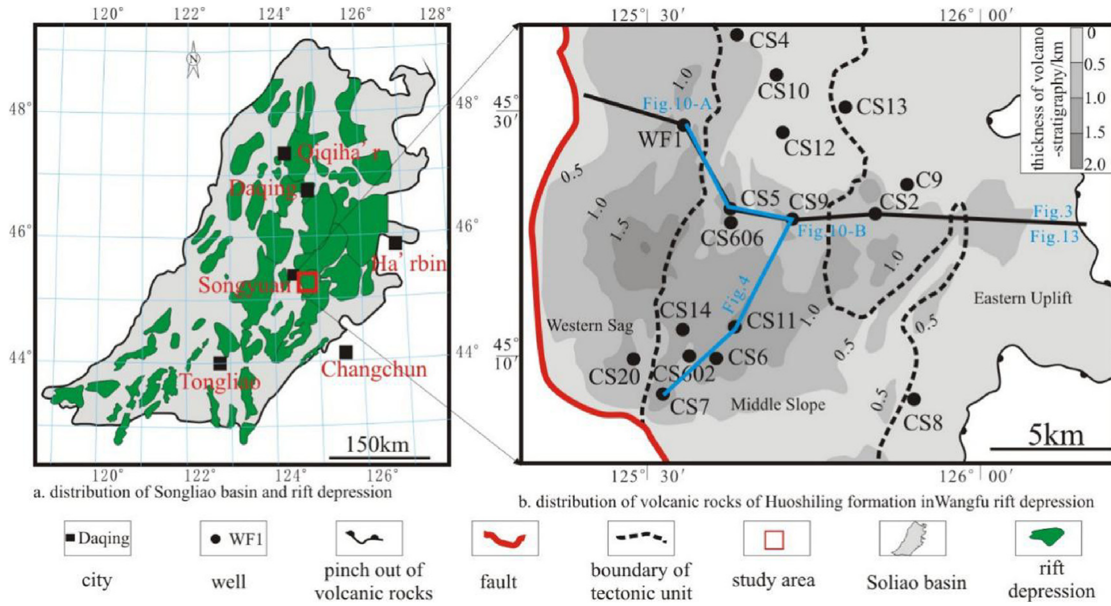

Fig. 2. Pilot map of the research area. Note: The thickness of the volcanostratigraphy of the Huoshiling Formation in the Wangfu Rift Depression is estimated based on both seismic and logging data.

analysis method of clay mineral relative content in sedimentary rocks".

Burial history analysis involved the determination of two denudation boundaries and closer examination of the burial history in wells WF1 and CS9. The acoustic time method was used to calculate the denudation thickness between the Nenjiang formation (early Campanian) and the Neogene. The denudation thickness of volcanic rocks in well CS9 was estimated using the surface trends of stratigraphic thickness. A burial curve was constructed based on the stratum lithology, the increase in compression with burial depth, and the stratum thickness.

The inclusion test was done at the Analytical Laboratory of BRIUG in Beijing, using the LINKAM THMS600, which was produced by Linkam Scientific Instruments Ltd, UK. The test method was performed according to the EJ/T 1105–1999 standard method, at a test temperature of 24 °C and relative air humidity of 40%.

4. Volcanostratigraphic characteristics

4.1. Filling

The volcanostratigraphy of the study area was formed in a half-graben basin during the early rifting stage of the Songliao Basin (Fig. 3). The seismic data shows that the maximum thickness of the basin fill is 1800 m. As a whole, the volcanostratigraphy comprises approximately 58% of the faulted part of the basin and 28% of the basin as a whole. From the thickness of the volcanic rocks, it is inferred that the volcanic centre is in the middle of the WRD. The seismic data shows that the volcanostratigraphic facies are tabular and partially mound-shaped interior reflections with weak amplitudes and low frequencies. However, due to the limited resolution of seismic data, the overlapping relationships are mostly unknown. Based on the trachyandesite associated with the Changbaishan volcano, the volcanostratigraphic formations are inferred to be mainly mounds with a large height to radius ratio related to widespread central eruptions (Tang et al., 2017b). Following deposition, the volcanostratigraphy experienced different burial stages that resulted in differing burial depths of the top boundary. The volcanic rocks near the western sag area experienced subsidence from the moment the basin was filled up to the middle Campanian. The volcanic rocks in the middle slope area experienced long-term denudation up until the early Berriasian followed by subsidence from the early Barrenmian to the middle Campanian. In the eastern uplift area, the volcanic rocks underwent uplift and long-term denudation from filling of the basin to the Albian, subsidence from the Cenomanian to the middle Campanian, uplift-related denudation in the later Campanian, and finally re-burial in the Neogene. This secondary burial however, was less than the maximum palaeoburial depth.

4.2. Composition

The base of the Huoshiling Formation in the WRD, found in the southern Songliao Basin, contains a thick unit of volcanic rocks. Drilling revealed that the maximum volcanic depth was in well CS7 at 1223 m (although the drill did not penetrate the entire unit). The cores of well CS11 and well CS603 reveal that the volcanic rocks are inclusive of the trachyandesite and trachyte (Fig. 4) which have been shown to be the main components of the volcanic units and comprise approximately 80% of the volume. The 15 wells that contain the volcanic rocks showed that the trachyandesite comprises approximately 51.3%, trachyandesitic ignimbrite comprises approximately 10.3%, and trachyandesitic tuff approximately 5.8% (Fig. 5). As well as these three main sub-groups there were also a few trachytes, andesitic pyroclastic rocks and tuffisites identified. The volcanostratigraphic filling sequence is divided into three types according to the thickness of the rock unit and the characteristics of well logging. The first type is the thick lava type, best represented in well CS7 that demonstrates thicknesses of a single layer up to 400 m, and show a gamma curve and density curve with a micro-jag low-amplitude block pattern. Second, the interbedded type represented in wells CS11 and WF1 that is overlapped by the ignimbrite and lava. The thickness of single layer is approximately 20–50 m, and the gamma and density curve have a medium-jag medium-amplitude block pattern. Third, the composite type represented in well CS9 and well CS5 that is overlapped by thick and thin layers of lava and/or ignimbrite.

4.3. EIUBs of volcanostratigraphy

The EIUBs are boundaries found within the volcano or as part of volcano and were formed during the eruption phases or epoch, with a time interval from years to thousands of years (Fisher and Schmincke, 1984; Tang et al., 2015). The marker beds for these EUIBs are the

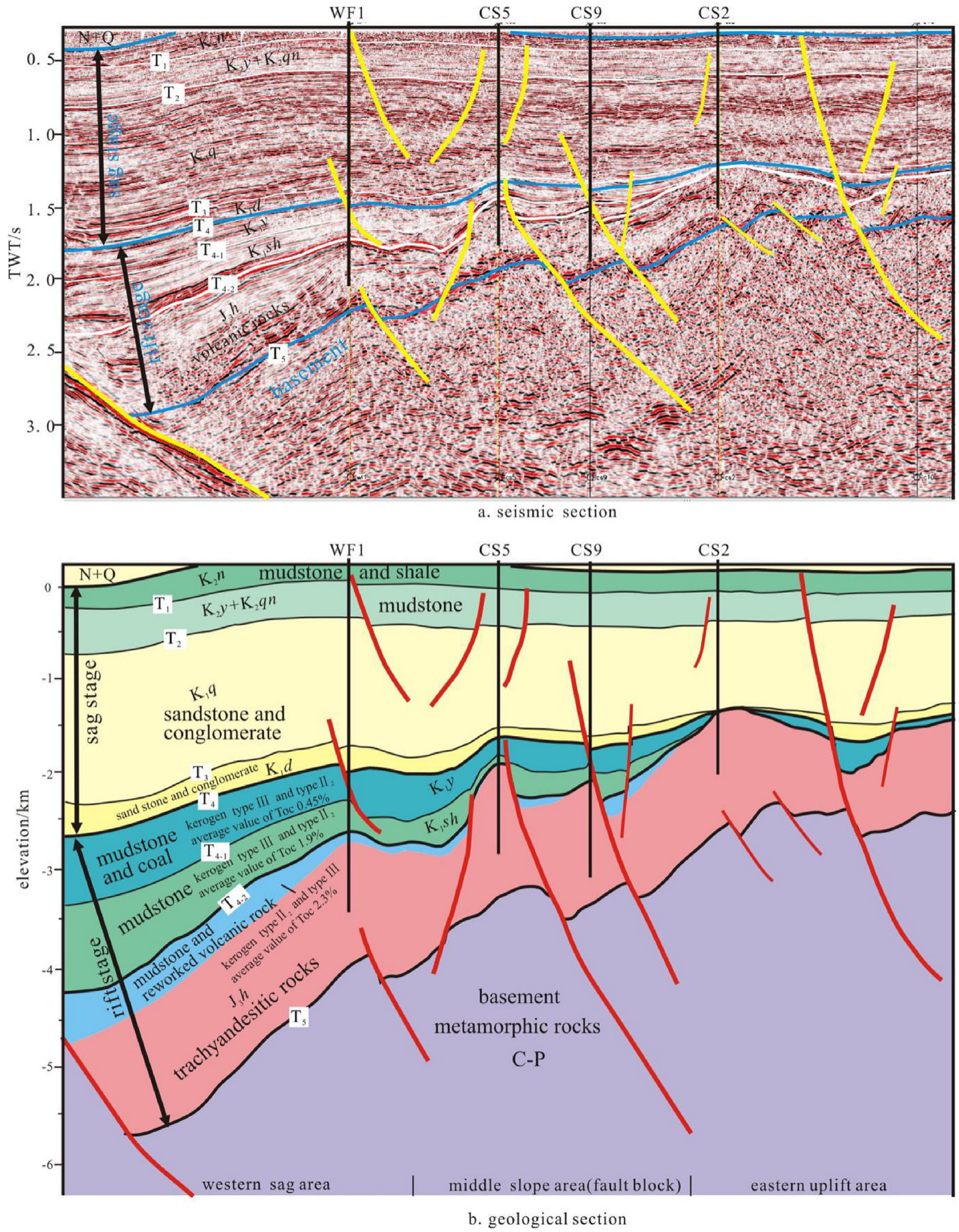

Fig. 3. The structural style and filling characteristics of the Wangfu Rift Depression, Songliao Basin, NE China. Notes: This Wangfu Rift Depression section shows the regional distribution of tectonic units. It is divided into 3 units: the western sag (WS), the middle slope (MS) with abundant normal faults, and the eastern uplift (EU). The time section is transferred into a depth section by using the acoustic time data (AC) and density log data. The volcanostratigraphy represents approximately 28% of the volume. The stratigraphic units are interpreted based on seismic facies units and are constrained by well lithologies. The kerogen and Toc data are from Zhang (2013). J_3h, Huoshiling Formation; K_1s, Shahezi Formation; K_1y, Yingcheng Formation; K_1d, Denglouku Formation; K_1q, Quangtou Formation; K_2qn, Qingshankou Formation; K_2y, Yaojia Formation, K_2n, Nengjiang Formation; C, Carboniferous; P, Permian.

reworked volcanic rocks or weathered crust and these allow the EUIBs to be identified. There are two types of filling sequences according to the EIUB. First, demonstrated by the volcanostratigraphy of 13 wells that have one EIUB that is found between the volcanic rocks and overlapping sedimentary rocks. There is no interbedding of sedimentary rocks which indicates that the volcanostratigraphy is in continuous construction, and that the time span that formed the volcanostratigraphy is relatively short. Secondly, the filling sequence with two EUIBs as in 2 wells (CS11 and WF1). The EUIBs form the top boundary of the volcanic rocks as well as a boundary between the interbedded sedimentary and volcanic rocks below (Fig. 5). The presence of the interbedded units indicates that the volcanostratigraphy in this type of EUIB is not continuous, and that the time span of volcanostratigraphy likely spans tens of thousands of years. In totally, the one or two EIUBs indicate that the thick volcanostratigraphy of WRD had been underwent the simple eruptive history.

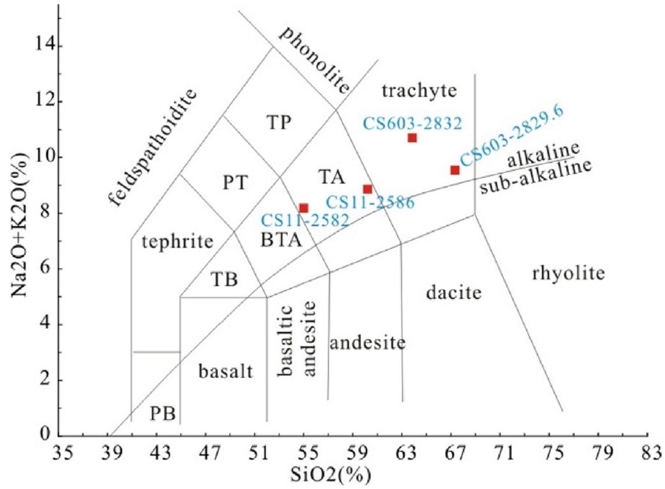

Fig. 4. TAS diagram of the volcanic rocks of Huoshiling Formation in the Wangfu Rift Depression, Songliao Basin, NE China, Notes: BTA-basaltic trachyandesite, PB-Picrite basalt, PT-phonolitic tephrite, TA-trachyandesite, TB-trachybasalt, TP-tephritic phonolite.

5. Types and characteristics of reservoir space

Based on observation of the cores, resin-impregnated sections and thin sections, the main reservoir space types in this area are primary pores, secondary pores and secondary fractures.

Primary pores consist mainly of amygdales and intergranular pores. The amygdales are usually found in the trachyandesite, and their distribution is limited. For example, the amygdales in well CS606 are 2 mm–5 mm in diameter, have elliptical shapes and demonstrate poor directionality. The filling degree is approximately 50–90%; having occurred in three filling stages, namely siliceous filling along the edges, chlorite filling the interior of the siliceous fill and calcareous filling in the centre (Fig. 6a/b). The intergranular pores are several millimetres in diameter, have irregular shapes and are understood to have undergone dissolution diagenesis or alteration diagenesis (Fig. 6c).

Secondary pores group together sieve pores and moldic pores. These pores develop in the intra-particle space or matrix in pyroclastic rocks and ignimbrites (Fig. 6c), while sieve pores are mostly present in the matrix in lava (Fig. 6d/e). The well segments with sieve pores are usually relatively unconsolidated. So pseudo-pores that form by the falling off of clay minerals can be found on the surface of cores (Fig. 6f). Moldic pores are usually formed by minerals such as hornblende and plagioclase that undergo alteration diagenesis and dissolution diagenesis in this volcanostratigraphic sequence (Fig. 6d/e). The observations of this study indicate that moldic pores could be an important contributor to porosity.

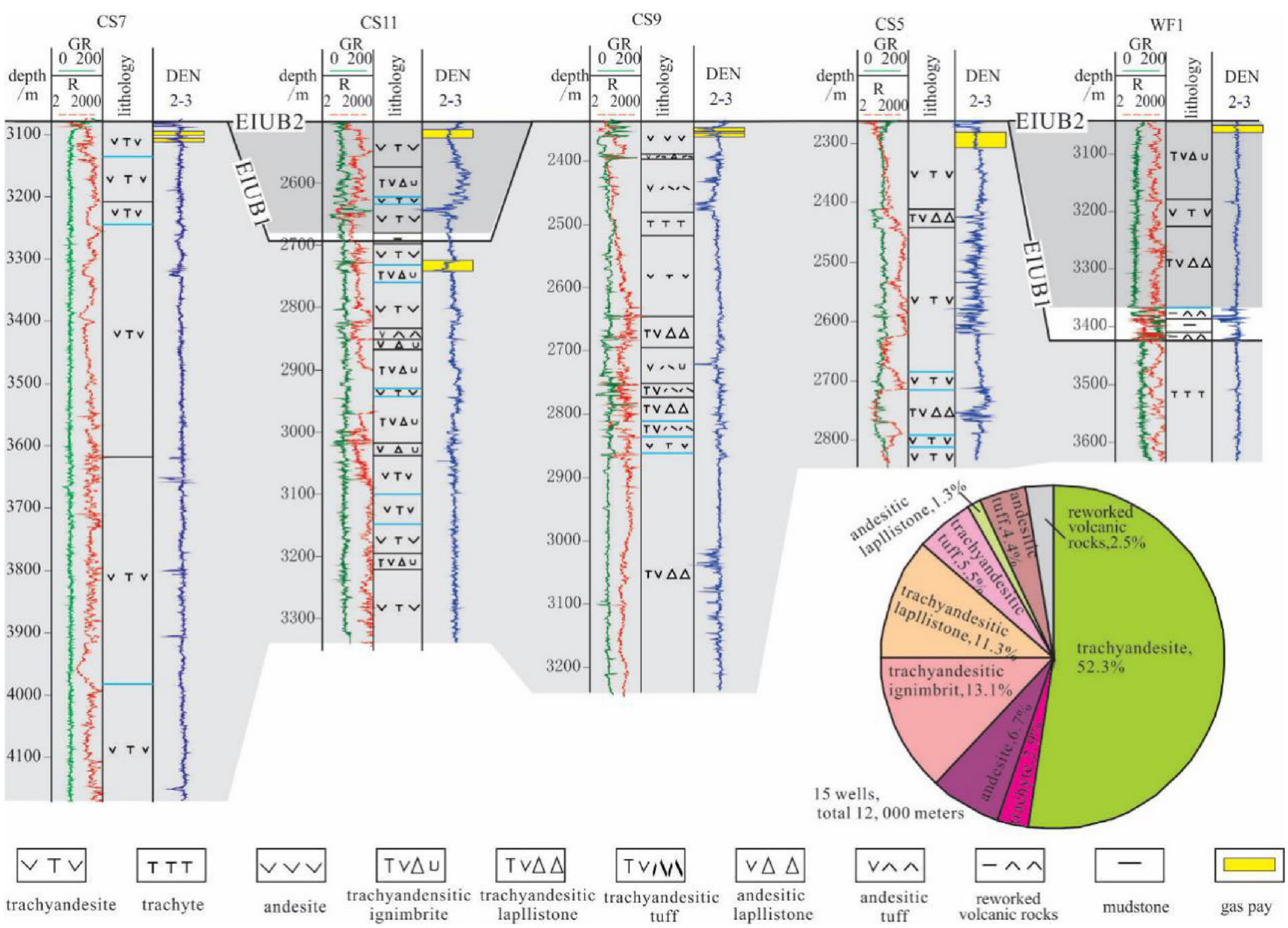

Fig. 5. Lithological and logging characteristics of the volcanostratigraphy of the Huoshiling Formation in the Wangfu Rift Depression, Songliao Basin, NE China. Notes: EIUB-eruptive interval unconformity boundary. The lithology is identified by using 40 m cores, 1200 cutting samples and FMI data. GR: natural gamma ray, API; R: Apparent resistivity from Computed Focusing Mode 5, Ω·m; DEN: density, g/cm^3.

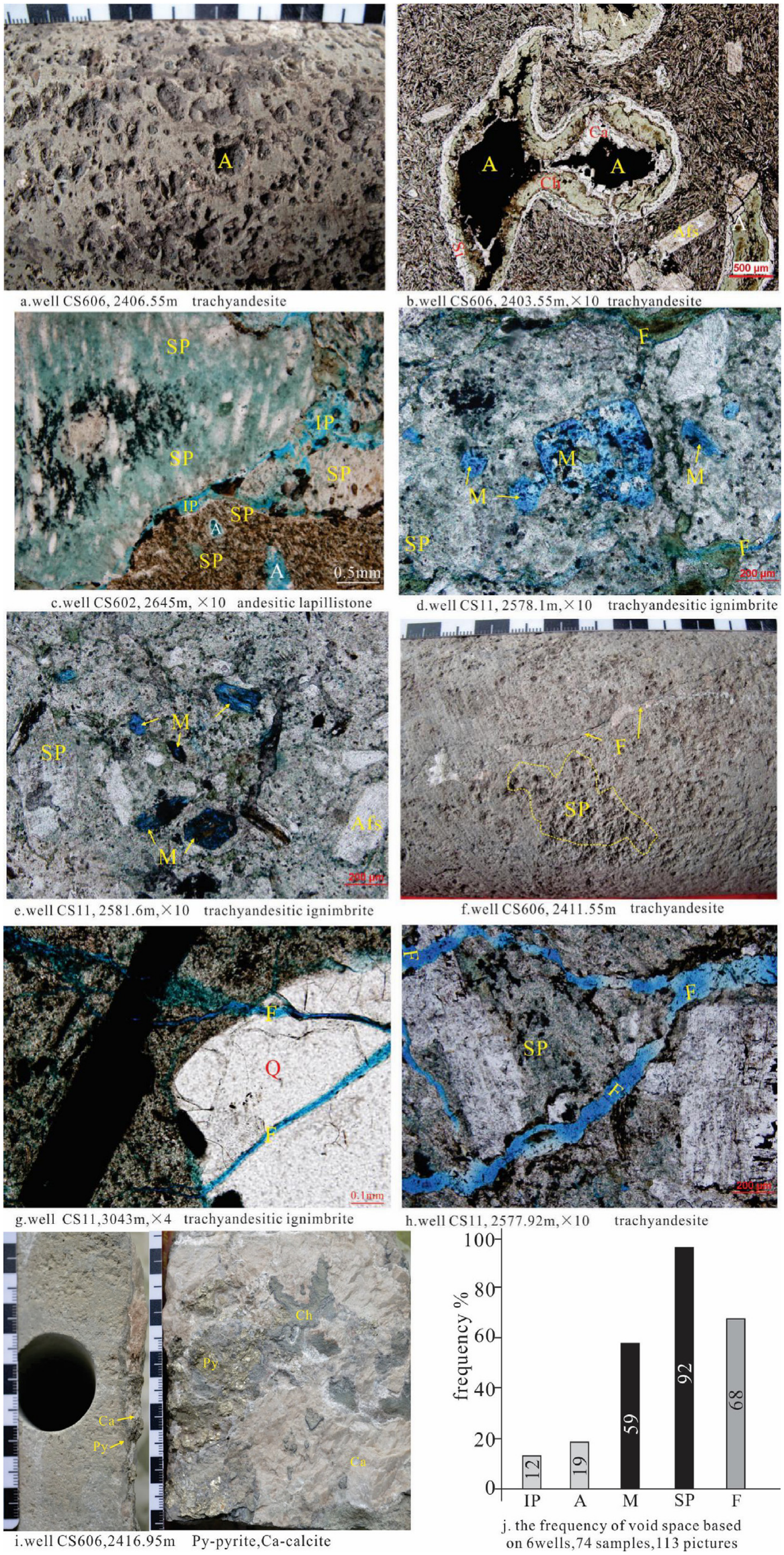

(caption on next page)

Fig. 6. Void space characteristics of the volcanostratigraphy of the Huoshiling Formation in the Wangfu Rift Depression, Songliao Basin, NE China. Notes: A-amygdale, IP-intergranular pore, M-moldic pore, SP-sieve pore, F-fracture; Afs-alkali feldspar, Ca-calcite, Ch-chlorite, Py-pyrite, Q-quartz, Si-siliceous material.

Secondary fractures consist mainly of tectonic fractures and weathering fractures. Tectonic fractures are formed by tectonic stresses and usually have regular shapes that will become irregular when diagenesis processes take place i.e. filling, alteration or dissolution (Olson et al., 2009; Jiang et al., 2017). The width of the tectonic fractures is commonly less than 1 cm and the filling degree is high in this volcanostratigraphy ca. 15–95% (Fig. 6g/h/i). The fractures are often filled with pyrite and calcite and some of the fractures have undergone alteration diagenesis.

Based on 113 pictures of 74 resin-impregnated sections and observations of 40 m cores from 6 wells, the prevalence of the reservoir space was analysed. The frequency of primary pores is relatively low, with intergranular pores and amygdales representing 12% and 19%, respectively. The frequency of secondary pores is relatively high, with moldic pores comprising 59% and sieve pores reaching 92% (Fig. 6j). As explained above, primary void space is relatively limited in this volcanostratigraphy, nevertheless secondary diagenesis produces abundant secondary pores and fractures that enhance the reservoir quality.

6. Reservoir distribution characteristics

6.1. Porosity, permeability and pore throat

There are 119 porosity & permeability values and 16 capillary pressure curve samples. Porosity values range from 0.3% to 16.7%, with an arithmetic average value of 8.3%; permeability ranges from 0.0004 mD to 93.78 mD, with an arithmetic average value of 5.55 mD (Fig. 7). In comparison to the sedimentary rocks, which exhibit medium-low porosity and permeability, the reservoir in this area can be well correlated with the rhyolitic rocks associated with high gas production in adjacent areas, such as the Qinsheng Gas Field and Songnan Gas Field (Feng, 2008; Tang et al., 2010). The ignimbrite presents the highest values of porosity and permeability, followed by pyroclastic rocks and then the lavas (Fig. 7b). The pore throat sizes have an average radius of 0.020–0.24 μm, middle-high displacement pressures, ranging from 1.15 to 19.69 MPa, and middle-high saturation values during mercury injection (from 49.31% to 98.46%) (Fig. 8).

6.2. Relationship between the reservoir and the EIUB

The relationship between the EIUB of each well and the porosity-permeability values associated, is analysed based on the lab data of core samples. Overall, the porosity and permeability of the lava, pyroclastic rocks and ignimbrite decreases with increasing distance from the EIUB of the volcanic rocks. The porosity and permeability change rapidly when it is apart from the boundary and can be split into four belts. Belt 1 demonstrates moderate values of porosity and permeability at about 40 m thickness. Belt 2 has the highest porosity and is also approximately 40 m thick. Belt 3, also demonstrates moderate porosity and permeability values but is slightly thicker than Belt 1 at about 60 m. Lastly, the lowest porosity and permeability belt, Belt 4, which is more than 180 m thick. From this information, it is concluded that the best quality of reservoir is Belt 2, which is situated approximately 40–80 m below the EIUB. Belts 1 and 3 that demonstrate moderate values of porosity and permeability are considered good reservoirs and are distributed approximately 0–40 m and 80–140 m below the EIUB respectively. Belt 4 is the least productive belt of the four and is found 140–320 m below the EIUB (Fig. 9).

Two EIUBs were identified at depths of 2530 m (EIUB1) and 2699 m (EIUB2). The casting thin sections, sidewall cores and FMI data indicated that the alteration degree and fracture density of the volcanic sequence decreased with increasing distance from the EIUBs.

First, detailed information on EIUB2 is outlined. The sidewall cores show that there are a few steep dip angles and regular smooth fractures. Additionally, the FMI data indicated that there were only a few moderate to steeply dipping angled fractures. The casting thin sections at depths of 2549.5 m and 2562.5 m showed that large areas of the matrix and many phenocrysts had undergone alteration, which had generated abundant sieve pores and moldic pores. The smaller matrix component at depths of 2549.5 m and 2562.5 m had also undergone alteration, but only sieve pores were generated here. This was also the case at depths of 2630 m and 2692 m surrounding fractures where small sieve pores were generated as a result of alteration. Amygdalae were observed, filled with chlorite and calcite at depths of 2617 m and 2660 m (Fig. 10a).

Second, detailed information on EIUB1 is introduced. The sidewall cores showed a few steep dip angles and regular smooth fractures. However, the FMI data indicated that there were few fractures. The

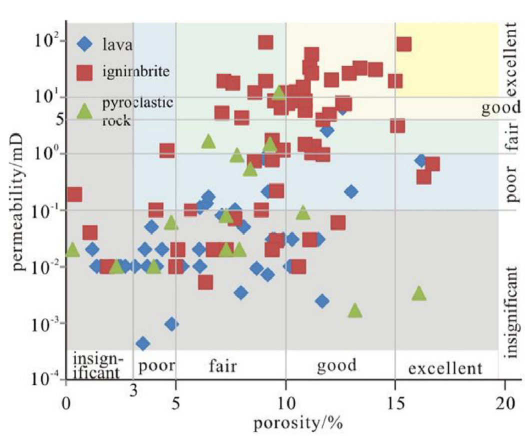

a.the crossplot of porosity and permeability

parameter		lava	ignimbrite	pyroclastic rock
porosity (%)	Min. value	1.2	0.4	0.3
	Max. value	16.2	16.7	16.1
	arithmetic mean	6.5	9.7	7.7
permeability (mD)	Min. value	0.0004	0.0053	0.001
	Max. value	6.30	93.78	11.80
	arithmetic mean	0.26	10.72	1.12
number of samples		45	59	15

b. statistic table of porosity and permeability

Fig. 7. Porosity characteristics of the volcanostratigraphy of the Huoshiling Formation in the Wangfu Rift Depression, Songliao Basin, NE China. Notes: Porosity values for gas reservoirs: insignificant, 0–3%; poor, 3–5%; fair, 5–10%; good, 10–15%; excellent, > 15%. Permeability values for gas reservoirs: insignificant, 0–0.1% mD; poor, 0.1–1 mD; fair, 1–5 mD; good, 5–10 mD; excellent, > 10mD. (From standard of the Petroleum Industry of the People's Republic of China (SY/T 6285-2011:“evaluating methods of oil and gas reservoirs”)). Lava includes trachyandesite, trachyte and andesite; ignimbrite includes trachyandesitic/andesitic ignimbrite; and pyroclastic rock includes trachyandesitic/andesitic pyroclastic breccia/lapillistone/tuff.

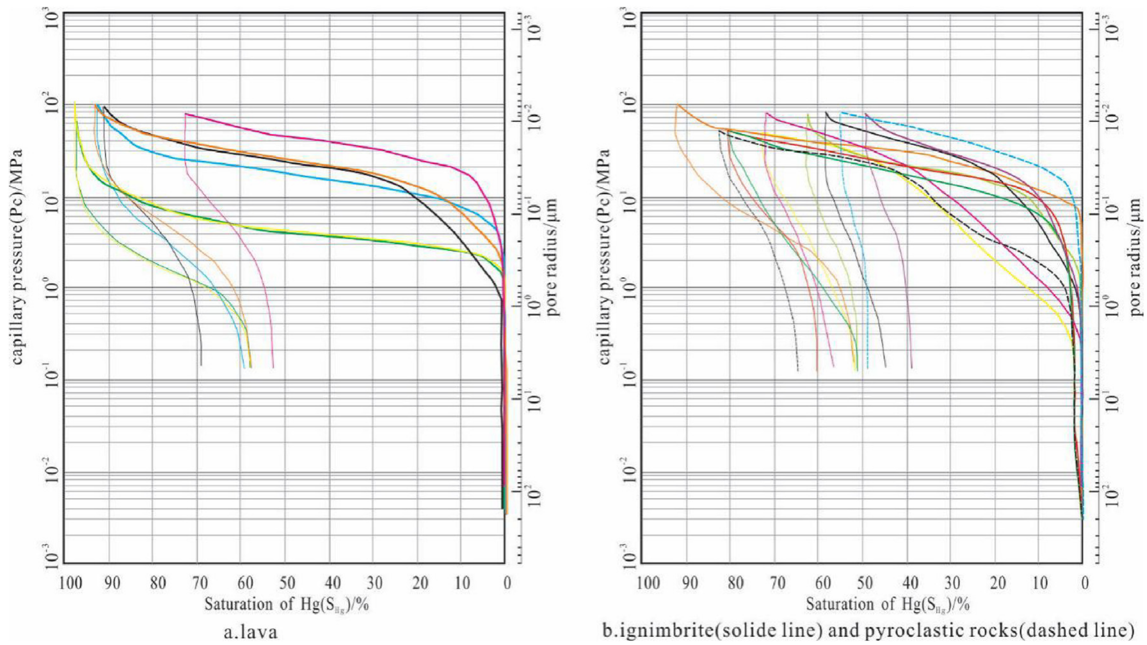

Fig. 8. Capillary pressure curve of lava, ignimbrite and pyroclastic rocks of the Huoshiling Formation in the Wangfu Rift Depression, Songliao Basin, NE China.

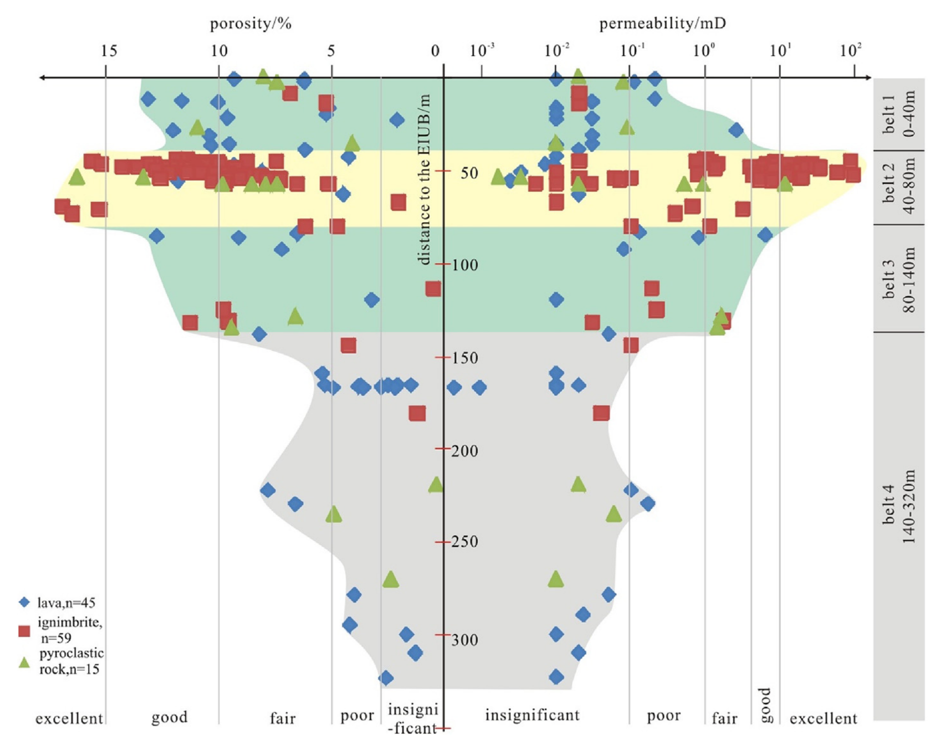

Fig. 9. Relationship between porosity-permeability and the EIUB of the Huoshiling Formation in the Wangfu Rift Depression, Songliao Basin, NE China. Notes: See Fig. 7.

casting thin sections at depths of 2699 m and 2720 m showed that large areas of the matrix and many phenocrysts had undergone alteration and that abundant sieve pores and moldic pores had been generated. Smaller areas of the matrix and many of the feldspars, at depths of 2765.0 m, 2767.0 m and 2769.0 m had undergone alteration, and sieve pores and moldic pores were generated. The void spaces were filled with calcite and quartz. A smaller proportion of the matrix and a few phenocrysts at depths of 2776.0 m and 2784.0 m had also undergone alteration, with sieve pores being generated (Fig. 10b).

The sidewall cores in well CS5 (Fig. 5), containing an EIUB, showed abundant netlike fractures with low filling degrees at depths of 2299–2320 m. However, there were a few regular and smooth micro-fractures present, with a high degree of filling at depths of 2321 m and 2423.9 m. The FMI data indicated that these netlike fractures were also present at depths of 2320–2360 m and could be divided into 2 types; those that are regular and smooth and those showing irregular fractures. The FMI data also indicated that only the regular and smooth fractures had high dip angles. From these observations it is inferred that the fracture density decreased with increasing distance of the volcanic rocks from the EIUB (Fig. 10c).

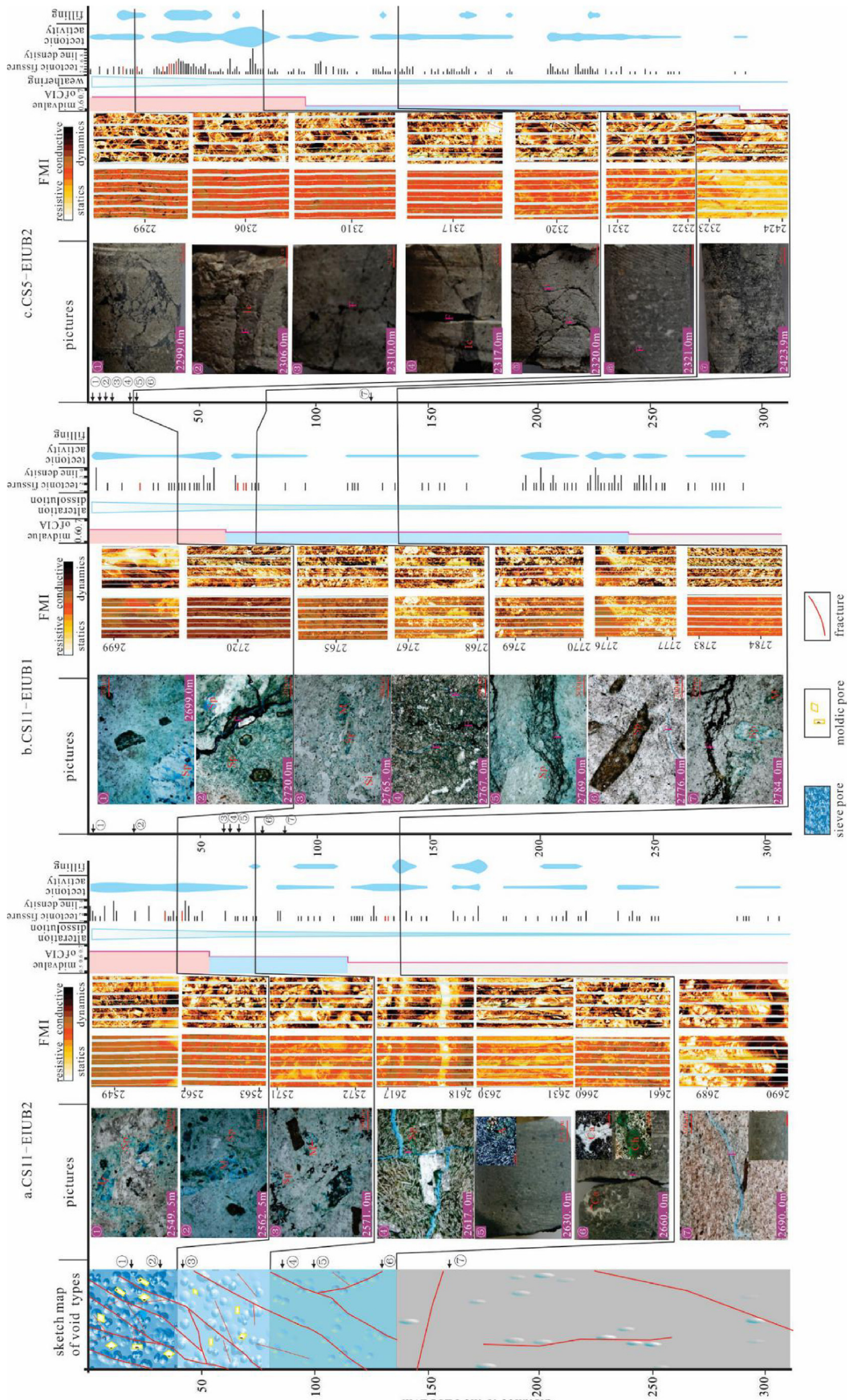

(caption on next page)

Fig. 10. The characteristics of void space in the thick volcanostratigraphy of the Wangfu Rift Depression in Songliao Basin, NE China. Notes: CIA = [Al_2O_3/(Al_2O_3 + CaO + Na_2O + K_2O)], oxide data from element capture spectroscopy (ECS). Density of tectonic fracture is estimated by using FMI, *n*/m; the high angle and regular fractures are the tectonic fractures. The red lines in tectonic fracture present the locations of sidewall cores. Filling degree correlates to the density of high resistance fractures (*n*/m). A-amygdale; M-moldic pore; SP-sieve pore; F-fracture, Si-siliceous material, Ca-calcite, Ch-chlorite. Ic-ichor, Ze-zeolite. (For interpretation of the references to colour in this figure legend, the reader is referred to the Web version of this article.)

7. Discussion

7.1. Reservoir formation

The formation of a volcanic reservoir is closely related to the kind of stratigraphic unit that it sits within, which will have an impact on the type of pore spaces (Sruoga et al., 2004; Rowe et al., 2012). For example, amygdales are associated with lava units, whereas intergranular pores are most commonly found in the pyroclastic units. The burial history following the formation of the stratigraphy is also important as it involves processes such as weathering and leaching during periods of exposure and deep-burial alteration that are important for the formation of secondary pores (Laubach and Ward, 2006; Sruoga and Rubinstein, 2007). Tectonic activities can also form secondary porosity, namely fractures. The details will be described below according to the reservoir type and characteristics.

7.1.1. Volatile matter released

The volatile components of magma, particularly H_2O, CO_2, F_2 and Cl_2, escape via degassing processes as the temperature and pressure decrease due to the ascent and migration of the magma (Gaonac'h et al., 2005; Lovejoy et al., 2004). Pores are created in the form of vesicles when bubbles are captured by a cooling magma, and amygdales form when these pores become filled by magma at a later stage of evolution, or by material rich in silica or calcium ions as a secondary process. The release and capture of volatile matter mainly occurs at the top of a lava flow, thus encouraging the development of a reservoir at the top of the stratigraphic sequence (Chen et al., 2016). However, diagenesis of this type is uncommon in the WRD, and amygdales are only observed in a few core sections (Fig. 6a and b), likely as a result of the low volatile content in the intermediate lavas.

7.1.2. Particle-support effect

When lava undergoes fragmentation, pyroclasts are generated in the form of blocks, bombs, lapillus and both coarse and fine grained ash (Fisher and Schmincke, 1984). Most of the pyroclasts are poorly-sorted and angular. The coarsest particles will form a stabilized skeleton first and then the fine particles will fall into the available spaces among the coarser particles. Intergranular pores form when the fine particles have a lower filling degree and thus leave some pore spaces empty (Klug and Cashman, 1996; Tang et al., 2016b). The particle-supported nature of coarse grains maintains the intergranular pores during the deep burial and compaction (Fig. 6c). Therefore, the ignimbrite and the pyroclastic deposits most likely have intergranular pores at depth because of particle-support effect.

7.1.3. Weathering and leaching

Weathering takes place when the volcanic rocks are exposed to atmospheric agents, such as water and wind, at or near the Earth's surface. The rocks can change colour, texture, composition, induration, or form, with little or no transport of the loosened or altered material. Water can selectively remove, or dissolve out any soluble constituents from a rock; a process known as leaching (Neuendorf et al., 2011). As well as water, microorganisms such as bacteria can enhance the alteration of rocks (Chen et al., 2014a,b). Weathering and leaching processes are important factors for the generation of secondary porosity (Mao et al., 2015).

The volcanic rocks of the Huoshiling Formation in the WRD experienced different burial stages. The three main areas representing these different burial histories are the eastern uplift area, the middle slope area and the western sag area. The eastern uplift and middle slope areas are similar in that they both experienced weathering and leaching, but they also exhibit some differences. For example, the eastern uplift area has different stratigraphy, i.e. it does not have the upper Huoshiling Formation, the Shahezi Formation and the Yingcheng Formation. Moreover, the wedge shape implies the paleo-slope during the Shahezi period and Yingcheng period and the strata overlapped from the west to east. Thus the eastern uplift area experienced long-term, likely more than 20 Ma, large-scale weathering and leaching. The middle slope area (as demonstrated in wells CS5 and CS9) is located in the volcanic highland formed in the footwall of a normal fault and the formation lacks the upper Huoshiling Formation and the lower Shahezi Formation. Based on the stratigraphic thickness, this volcanic highland would also have experienced weathering and leaching for millions of years (Fig. 11). The weathering and leaching processes mean that the reservoir distribution is closely related to the EIUB because they influence the reservoirs development at the top of the thick volcanostratigraphic sequence. Below the EIUB in well CS5, the closer to the boundary, the higher the fracture density was. The upper part of the same well had netlike fractures while the lower part had only high dip angle fractures (Fig. 10). Weathering and shrinkage processes are likely the main contributors to the generation of netlike fractures in the upper part of CS5. The weathering fractures were generated when the volcanic rocks were uplifted and exposed and the shrinkage fractures or tectonic fractures become enlarged due to alteration from meteoric water (Tang et al., 2016a). These secondary fractures could also have been an important contributor to the overall porosity.

7.1.4. Burial alteration

During thermal evolution, organic matter in the mudstones and coal seams produces organic acid, CO_2 and CH_4, among other compounds, which lead to alteration of the volcanic rocks. Large quantities of this organic acid are usually produced during two stages in coal bearing strata. Firstly, the process of turning plant remains into peat and lignite within a burial depth range of 200–400 m can produce pH values as low as 3.3–4.6 (Zheng and Ying, 1997; Zhong et al., 2003). Secondly, acids discharged by mudstones and coal seams during the thermal evolution of organic material (70–170 °C) can significantly decrease the pH values of any water already in the formation, thus allowing material to be further altered by acid (Liu et al., 1998; Yang et al., 2004; Zhang et al., 2011). This process produces the sponge pores, sieve pores, cave and moldic pores via alteration and dissolution (David and Walker, 1990; Blum and Stilling, 1995; Sruoga and Rubinstein, 2007).

The volcanic rocks of well CS9 have hydrocarbon-bearing inclusions found in secondary quartz (Fig. 12). This indicates that the volcanic rocks have undergone burial alteration by organic acid or CO_2 during thermal evolution. The organic acid or CO_2 probably came from the overlying source rocks, such as mudstones (kerogen Type II_2 and type III, Toc 0.4–2.5%) and coal, that is evidenced by the boreholes (Zhang, 2013). The wells do not penetrate the Huoshiling Formation and thus cannot reveal the lower part of the sequence. However, the probability of any source rocks in the bottom part is limited because of chaotic and low frequency seismic facies (Fig. 3). The volcanic rocks of the Huoshiling Formation in the WRD contain easily altered components, such as feldspar, glassy debris and ash etc., which may play an important role in the origin of secondary pores. As shown in Fig. 6, four types of alteration phenomena can produce pores. Sponge-like pores are produced through trachyandesitic debris alteration (Fig. 6c), moldic

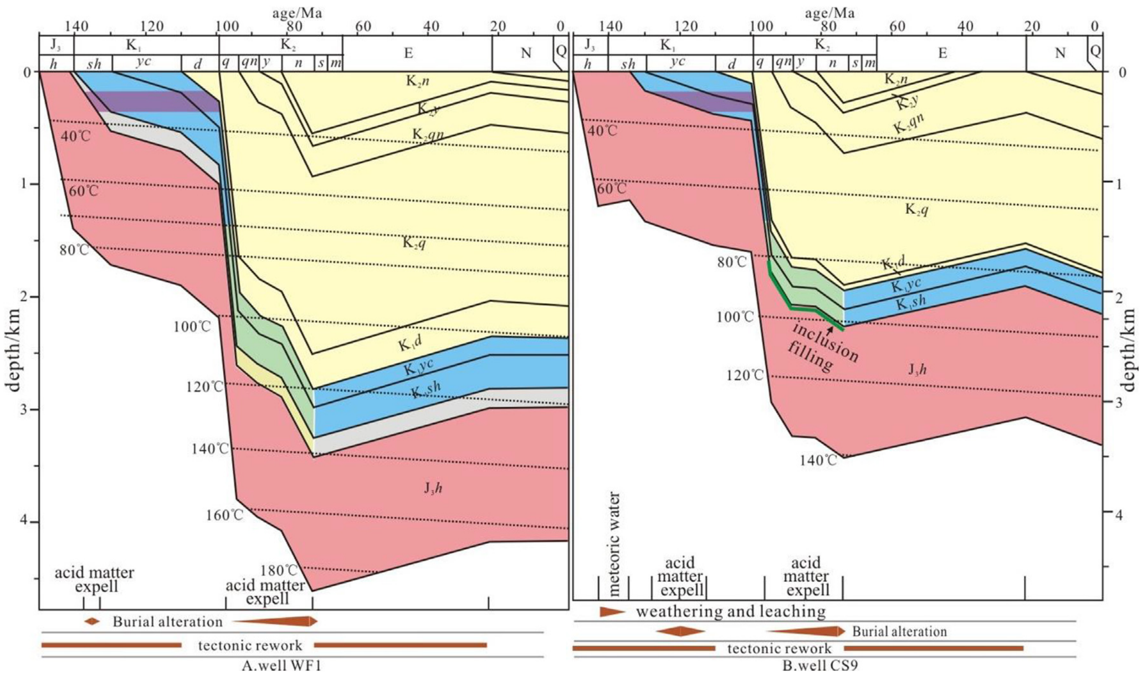

Fig. 11. The burial history of well WF1 and well CS9 in the Wangfu Rift Depression, Songliao Basin, NE China. Note: The present formation temperature is based on the results of 20 well tests with depths between 1500 and 3000 m. The palaeotemperature in the late Cretaceous is based on fluid inclusion microthermometry data and clay mineral transformation data from well Z12 and well S5 (Ren et al., 2001). The unrevealed thickness of volcanic rocks is estimated by using seismic, AC and density logging data. The consolidation of the sedimentary stratigraphy is estimated by using the normal consolidation line (Allen and Allen, 2013). The consolidation of the volcanostratigraphy is not estimated. J_3h, Huoshiling Formation; K_1s, Shahezi Formation; K_1y, Yingcheng Formation; K_1d, Denglouku Formation; K_1q, Quangtou Formation; K_2qn, Qingshankou Formation; K_2y, Yaojia Formation, K_2n, Nengjiang Formation.

pores are produced by hornblende alteration (Fig. 6e) and some sponge-like pores are produced by trachyandesitic matrix alteration (Fig. 6d/h). The moldic pores and sieve pores that were formed by alteration tend to be larger in diameter, whereas the sponge-like pores are smaller. Together, these pores result in a reservoir characterized by high porosity and small throats. Based on the microthermometric results of hydrocarbon-bearing inclusions in well CS9, it is seen that most of the inclusions exhibit peak temperatures of 90–107 °C, which were reached during the Cenomanian to Campanian according to the burial history (Figs. 11 and 12). Therefore, the reservoir formation age is equal to or older than the inclusion charging age.

The results of X-ray analysis indicate that the volcanic clay minerals in the depression and slope areas are mainly chlorite with small amounts of illite and smectite (Table 1). The reason for this is as follows. On one hand, chlorite could have been formed as a result of the hornblende alteration process during deep burial. This is seen in the fractured and crushed amphibolite found in the crater area, where the amphibolite has been strongly altered and replaced with secondary chlorite minerals. The chloritic mineral assemblage suggests formation temperatures of 100–300 °C (Kirsimae et al., 2002) which is important because the controlling factor of chlorite formation is the temperature (Inoue et al., 2009; Bourdelle and Cathelineau, 2015). The maximum palaeotemperature of the volcanostratigraphic sequence in this area is 135–190 °C. Therefore, the temperature conditions would have been suitable for clay minerals to be transformed into chlorite. The other dominant process that likely occurred is the alteration of feldspars to clay minerals. When the rocks were exposed at the Earth's surface, feldspar phenocrysts as well as feldspars in the matrix would have weathered into clay minerals, such as montmorillonite and kaolinite, which would have been transformed to illite as the burial depth increased (Cathelineau and Izquierdo, 1988; Battaglia, 2004; Noguera et al., 2011). Only when the amounts of Fe and Mg ions were sufficient,

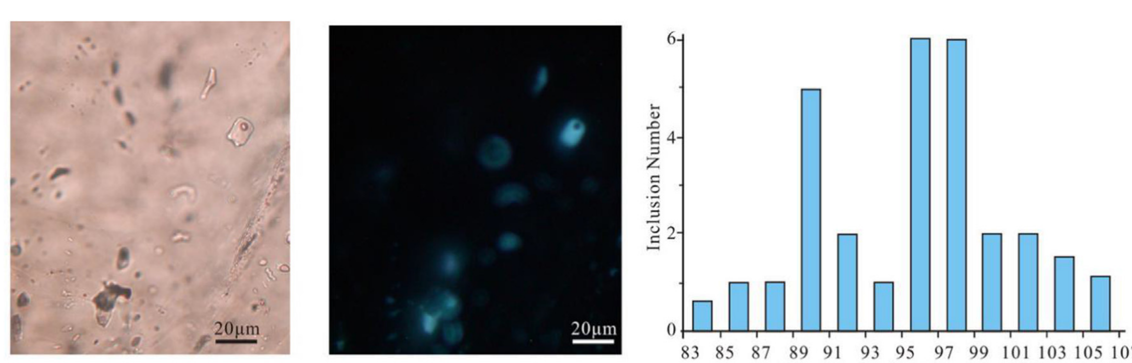

(a) Inclusions of well CS9 at 2268.0m (plane-polarized light) (b) Inclusions of well CS9 at 2268.0m (UV fluorescence) (c) Inclusion Homogenization Tempreture

Fig. 12. Characteristics and homogenization temperatures of hydrocarbon-bearing inclusions of Well CS9 in the Wangfu Rift Depression, Songliao Basin, NE China. Notes: (a) and (b): Hydrocarbon-bearing inclusions located in micro-factures in quartz crystals.

Table 1
Characteristics of mineral compounds in the volcanic rocks of the Huoshiling Formation in the Wangfu Rift Depression.

Well	Depth	Distance to the EIUB (m)	Mineral species and content (%)								Total clay mineral content (%)	Relative amount of clay mineral (%)			
	(m)		Q	Kfs	Ab	Cal	Dol	Am	Ap	Lmt		I/S	I	K	C
CS11	2577	27	4.3	10.8	65.4	1.1	/	/	/	4	14	3	3	/	94
CS11	2579	29	1.7	3.3	56.1	3.6	/	/	/	19.1	16	/	/	/	100
CS11	2583	33	23	12.7	45.3	1.1	/	1.5	/	5.4	11	/	/	/	100
CS11	2585	35	36	6	41	2	/	/	/	/	15	4	6	/	90
CS11	2588	38	/	8.6	53.5	1.1	/	1.4	/	10.4	25	/	/	/	100
CS606	2409	49	9.2	9.8	46.1	7	/	/	5.3	/	23	/	1	/	99
CS606	2410	50	/	10	86	/	/	/	/	/	4	/	/	50	50
CS606	2413	53	/	1	97	/	/	/	/	/	2	/	/	100	/
CS606	2414	54	/	5.2	42.7	18.1	/	/	4.6	/	29	/	4	/	96
CS606	2417	57	/	3.2	53.1	/	/	/	6.9	/	37	/	1	/	99
WF1	3590	160	27	7	56	/	/	/	/	/	10	6	9	/	85

Notes: Kfs = K-feldspar, K = Kaolinite, Pl = Plagioclase, Ab = Albite, Chl = Chlorite, Cal = Calcite, Dol = Dolomite, Am = Amphibole, Ap = Apatite, Lmt = Laumontite. The two samples that have a higher quartz content (23%–26%) are filled by silica in well CS11 and the sample with the higher calcite content (18.1%) is filled by calcium in well CS606.

would the illite transform into chlorite. The fractures in well CS6 were filled with pyrite. This finding indicates that a Fe-rich fluid had been present in the post-volcanic period. The above conditions were beneficial for the transformation of illite and kaolinite into chlorite. These factors were primarily responsible for the alteration of clay minerals to chlorite (Li et al., 1988; Huang et al., 2003, 2009; Wang et al., 2005). The dissolved pores in this area not only contributed to the high porosity but also produce a relatively suitable connectivity (i.e., high permeability) (Cai et al., 2010; Luo et al., 2012, 2013; Zhang et al., 2012; Wang et al., 2013).

The number of secondary pores decreased with increasing distance of the volcanic rocks from EIUB1 and EIUB2 in well CS11. Due to the migration of dissolved fluids from the overlying strata into the volcanic rocks of the Huoshiling Formation below, the top most section of the volcanic rocks dissolved sooner, which enhanced the reservoir quality in this area (Fig. 13). Moreover, because of the different burial depths of the volcanic rocks in the Huoshiling Formation, the degree of thermal evolution differs among the eastern uplift, middle slope and western sag (Fig. 13). The western sag turned into a mature area in terms of organic matter evolution (Figs. 11 and 13) in the early Aptian to early-middle Campanian, and deep-burial alteration occurred in the early Aptian to middle-late Campanian. The slope area reached maturation in terms of organic matter evolution between the Turonian and the middle Campanian, and deep-burial alteration occurred in the Turonian to middle-late Campanian. The overlying strata of the Yingcheng Formation in the eastern uplift area turned into a mature area in terms of organic matter evolution between the Coniacian and the late Campanian, and deep-burial alteration occurred in the Coniacian to middle-late Campanian. Therefore, the duration of deep-burial alteration in the depression was longer than the duration of deep-burial alteration in the uplift area.

7.1.5. Tectonism

The tectonic activity in the region is important because it will generate tectonic fractures that may contribute to the overall porosity and permeability of the area. The volcanostratigraphy of the Huoshiling Formation in the WRD experienced two main tectonic episodes. The first episode produced fractures related to the effects of block faulting during the Tithonian to the Hauterivian. The tectonic effects on the volcanostratigraphy of the basin are very complicated due to the long duration of faulting. Extensional tectonism likely generates the net-like and irregular fractures (Fig. 6h/Fig. 10a-④/c-⑤). Fig. 6-h shows that the fractures in the slope area became filled with siliceous material at some later stage. Subsequently, the volcanostratigraphy of the WRD experienced compressional tectonism and tectonic inversion during the Nenjiang stage (Figs. 3 and 11), which also produced tectonic fractures. The high-angle fractures are likely related to the tectonism during this stage (Fig. 6i). Moreover, the fractures in the cores are generally less common than secondary pores (Fig. 6j) and are mostly closed under the burial conditions meaning that their contributions to porosity are limited. However, they do increase the connectivity of other void spaces and improve the permeability of the reservoir.

7.2. Main controlling factors of reservoir and exploration significance

The thickness of the most effective reservoir in boreholes found in the eastern uplift area and middle slope area, which experienced weathering and leaching, is relatively large, ranging from 21.5 to 59.5 m. The thickness of the effective reservoir in boreholes of the middle slope area and western sag area, which only experienced deep-burial alteration, is relatively small, ranging from 20 to 22 m (Table 2). From this information it is inferred that weathering and leaching had the largest impact on the reservoir in this area.

The gas daily production data suggests that weathering and leaching is necessary to produce a commercial gas pool especially in the boreholes in the middle slope that have a better accumulation effect. The boreholes in the western sag area and middle slope that have only undergone deep-burial alteration are poorly productive.

The area most impacted by weathering and leaching should correlate to the volcanic inherited-uplift areas that are likely to form the structural traps that are better for gas accumulation. The area that only underwent deep-burial alteration should correlate to the stable subsidence area in the WRD which is not ideal for gas accumulation (Fig. 13). Therefore, the best exploration target area in the thick volcanostratigraphy in the WRD is the volcanic uplift area, particularly near the source rocks.

Above all, the best exploration target area should be the volcanic uplift region in the middle slope area due to four favourable factors: good reservoir quality (several Ma weathering-leaching), proximity to source rocks, proximity to fluid migrating at the channel, and wide distribution of the regional seal rocks (i.e., the mudstone of Shahezhi Formation and Yingcheng Formation). The second best exploration target region is the uplift area in the western sag also due to its four favourable factors: good reservoir quality (couple Ma weathering-leaching and strong deep-burial alterations), wrapped by source rocks, short distance of migration of hydrocarbons, and wide distribution of regional seal. The third best exploration target area is the eastern uplift because of its good reservoir quality (20 Ma weathering-leaching, indicating the higher secondary porosity). However, the unfavourable factors of this area include the long distance of gas migration and the poor seal. Thus, the sequence of best exploration target areas is as follows; the volcanic inherited-uplift zone in middle slope area, then the inherited palaeohighs of the western sag and finally the eastern uplift

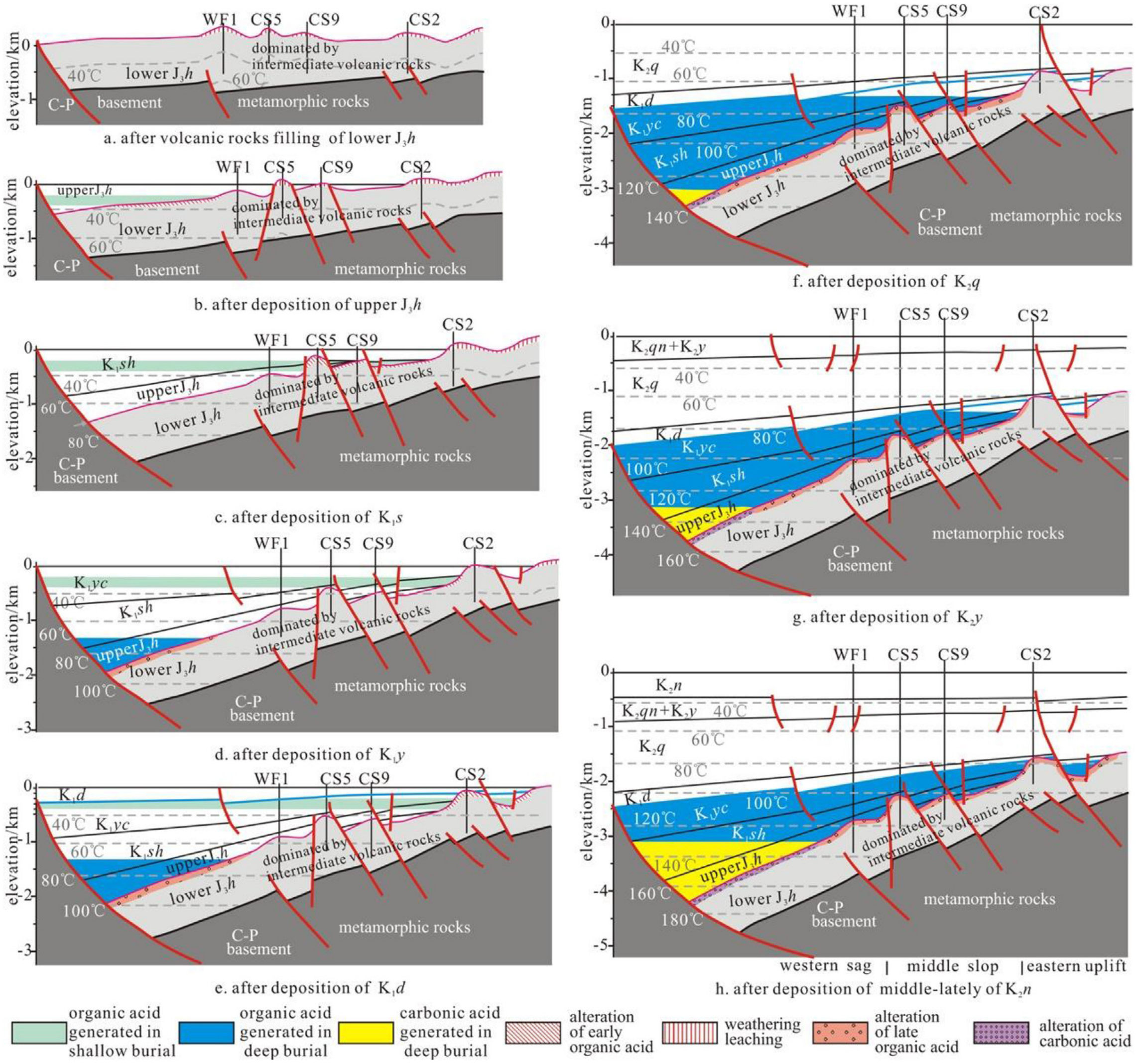

Fig. 13. The evolution of the volcanic reservoir of the Wangfu Rift Depression in Songliao Basin, NE China. Note: J_3h, Huoshiling Formation; K_1s, Shahezi Formation; K_1y, Yingcheng Formation; K_1d, Denglouku Formation; K_1q, Quangtou Formation; K_2qn, Qingshankou Formation; K_2y, Yaojia Formation, K_2n, Nengjiang Formation; C, Carboniferous; P, Permian. The present formation temperature is based on the results of 20 well tests with depths between 1500 and 3000 m. The palaeo-temperature in the late Cretaceous is based on fluid inclusion microthermometry data and clay mineral transformation data from well Z12 and well S5 (Ren et al., 2001).

Table 2
Lithology, location, reservoir characteristics and gas production of the Huoshiling Formation in the Wangfu Rift Depression.

Well	Lithology	Location	Reservoir formation	Daily output		Effective reservoir layer/thickness (m)	Gas PI equivalence (m^3/d·m)	Gas PI (m^3/d·m)
				Gas (m3)	Water (m^3)			
CS2	Trachyandesitic breccia	EU	WL, PS, AOA	12950	24	1/21.5	1728	602
CS13	Brecciated trachyandesite	EU	WL, PS, AOA	2100	142	2/28.5	5063	74
C9	Trachyandesitic breccia	EU	WL, PS, AOA	0	80	1/30.0	2697	0
CS8	Trachyandesite	EU	WL, AOA	0	120	4/50.0	2400	0
CS4	Trachyandesite	MS	AOA	3000	12	2/22.0	682	137
CS5	Trachyandesite	MS	WL, AOA	73860	19	2/26.7	3485	2766
CS6	Trachyandesite	MS	WL, AOA	154790	0	2/30.9	5009	5009
CS7	Trachyandesite	MS	WL, AOA	10860	20	3/59.5	518	182
CS11	Trachyandesite	MS	VMR, WL, AOA	50750	135	2/31.0	3388	1637
CS12	Trachyandesite	MS	AOA	1500	30	2/21.0	1500	71
WF1	Trachyandesitic brecciated lava	WS	AOA, WL, PS	16900	70	2/36.6	2372	462
CS20	Trachyandesite	WS	AOA	100	40	1/20.0	405	5

Notes: WS-western sag, MS-middle slope, EU-eastern uplift; PS-particle-supported, WL-weathering and leaching, AOA-alteration by organic acids, VMR-volatile matter released; PI-productivity index, Gas PI equivalence =(gas daily output + water daily output × 1000)/effective reservoir thickness. The daily output is announced by E&P Research Institute of PetroChina Jilin Oilfield.

area (Table 2).

8. Conclusions

(1) The intermediate volcanic rocks of the Huoshiling Formation form a thick layer in the WRD. The filling sequences of the volcanic rocks were divided into three types according to the thickness of the rock layer and the well logging characteristics, namely, a thick lava type (the thickness of a single layer was up to 400 m), an interbedded type (the thickness of a single layer ranged from 20 to 50 m), and a composite type (overlapping thick and thin layers). Most of the boreholes revealed that the volcanic stratigraphic unit experienced only one construction stage, although a few boreholes revealed two construction stages with an interval between the two construction stages lasting tens of thousands of years.

(2) The thick volcanic rocks of the Huoshiling Formation in the Wangfu Rift Depression exhibited mostly low to moderate porosity and permeability values. The intermediate volcanic rock layers and reservoir distributions were closely related to the EIUBs. The core and FMI data revealed that the fracture density development and number of secondary dissolved pores (matrix spongy, phenocryst moldic and cribriporal pores) increased with increasing distance from this boundary. The cores showed that many of the favourable reservoirs were located approximately 40–80 m below the EIUBs. The quality of the reservoirs in Belt 1 and Belt 3, distributed approximately 0–40 m and 80–140 m below the EIUB respectively, was deemed suitable. The quality of the reservoirs in Belt 4, which was distributed 140–320 m below the EIUB, however, was only fair.

(3) The void spaces of thick volcanic rocks of the Huoshiling Formation in the Wangfu Rift Depression were generated by the release and capture of volatile matter, particle-supported effects, weathering and leaching processes and deep-burial alterations. The weathering and leaching processes were the key controlling factors of the reservoir quality followed by deep-burial alteration diagenesis according to a comparison analysis between the diagenesis and gas production index equivalence.

(4) The best exploration target areas of the thick volcanic rocks in the half-graben basins were the upper parts of the inherited volcanic highlands in the middle slope area, followed by the inherited palaeohighs of the sag area, and finally the inherited palaeohighs of the uplift area.

Acknowledgments

We thank Dr Zhao Ranlei, Yu Taiji, Kong Tan, Yang Di, and Li Jianhua for sample collection and laboratory testing. We also thank 3 anonymous reviewers for their experienced insights. We thank Georgie Rule and Phiri Cryton for careful review. This study was supported by the Major Program of the National Natural Science Foundation of China (41790453), the Natural Science Foundation of Jilin Province (20170101001JC), the National Natural Science Foundation of China (41472304), and the National Science and Technology Major Project of the Ministry of Science and Technology of China (2016ZX05026-004-001).

Appendix A. Supplementary data

Supplementary data to this article can be found online at https://doi.org/10.1016/j.marpetgeo.2019.104128.

References

Allen, P.A., Allen, J.R., 2013. Basin Analysis. Wiley-Blackwell.

Antonio, P., Giovanni, C., Nicoletta, F., Valentina, B., Gianluca, N., 2012. Influence of alteration on physical properties of volcanic rocks. Tectonophysics 566–567 (2012), 67–86.

Battaglia, S., 2004. Variations in the chemical composition of illite from five geothermal fields: a possible geothermometer. Clay Miner. 39, 501–510.

Blum, A.E., Stilling, L.L., 1995. Feldspar dissolution kinetics. In: White, Brantley (Ed.), Chemical Weathering Rates of Silicate Minerals. Reviews in Mineralogy, pp. 31.

Bourdelle, F., Cathelineau, M., 2015. Low-temperature chlorite geothermometry: a graphical representation based on a T–R^{2+}–Si diagram. Eur. J. Mineral. 27 (5), 617–626.

Cai, D.M., Sun, L.D., Qi, J.S., Dong, J.H., Zhu, Y.K., 2010. Reservoir characteristics and evolution of volcanic rocks in Xujiaweizi fault depression. Acta Pet. Sin. 31 (3), 400–407 (in Chinese with English abstract).

Cai, Z.R., Huang, Q.T., Xia, B., Lü, B.F., Liu, W.L., Wan, Z.F., 2012. Development features of volcanic rocks of the Yingcheng Formation and their relationship with fault structure in the Xujiaweizi fault depression, Songliao Basin, China. Pet. Sci. 9 (4), 436–443.

Cao, Y.C., Jiang, Z.X., Qiu, L.W., 1999. Study on the type and origin of the reservoir space of igneous oil reservoir in Shang 741 block, Huimin depression, Shandong. Acta Petrol. Sin. 15 (1), 129–136 (in Chinese with English abstract).

Cathelineau, M., Izquierdo, G., 1988. Temperature — composition relationships of authigenic micaceous minerals in the Los Azufres geothermal system. Contrib. Mineral. Petrol. 100 (4), 418–428.

Chen, H.Q., Hu, Y.L., Jin, J.Q., Ran, Q.Q., Lin, Y., 2014a. Fine stratigraphic division of volcanic reservoir by uniting of well data and seismic data—taking volcanic reservoir of member one of Yingcheng Formation in Xudong area of Songliao Basin for an example. J. Earth Sci. 25 (2), 337–347.

Chen, Z.H., Wang, X.L., Zha, M., Zhang, Y.Q., Cao, Y.C., Yang, D.S., Wu, K.Y., Chen, Y., Yuan, G.H., 2017a. Characteristics and formation mechanisms of large volcanic rock oil reservoirs: a case study of the Carboniferous rocks in the Kebai fault zone of Junggar Basin, China. AAPG (Am. Assoc. Pet. Geol.) Bull. 100 (10), 1585–1617.

Chen, Z.H., Liu, W., Zhang, Y., Yan, D.T., Yang, D.S., Zha, M., Li, L., 2016. Characterization of the paleocrusts of weathered Carboniferous volcanics from the Junggar Basin, western China: significance as gas reservoirs. Mar. Pet. Geol. 77, 216–234.

Chen, Z.H., Wang, X.Y., Wang, X.L., Zhang, Y.Q., Yang, D.S., Tang, Y., 2017b. Characteristics and petroleum origin of the Carboniferous volcanic rock reservoirs in the Shixi Bulge of Junggar Basin, western China. Mar. Pet. Geol. 84, 517–537.

Chen, Z.Y., HY, Li, J.S., Zhang, G., Zhang, Z.W., Liu, B.Z., 1999. Relationship between tertiary volcanic rocks and hydrocarbons in the Liaohe Basin, People's Republic of China. AAPG (Am. Assoc. Pet. Geol.) Bull. 83, 1004–1014.

Chen, S., Wu, Z.J., Peng, X.T., 2014b. Experimental study on weathering of seafloor volcanic glass by bacteria (Pseudomonas fluorescens) – implications for the contribution of bacteria to the water–rock reaction at the Mid-Oceanic Ridge setting. J. Asian Earth Sci. 90, 15–25.

David, F., Walker, L., 1990. Ion microprobe study of intragrain micropermeability in alkali feldspars. Contrib. Mineral. Petrol. 139, 17–35.

Einsele, G., 2000. Sedimentary Basins. Springer, Berlin.

Feng, Z.H., Shao, H.M., Tong, Y., 2008. Controlling factors of volcanic gas reservoir property in Qingshen gas field, Songliao Basin. Acta Geol. Sin. 82 (6), 760–768 (in Chinese with English abstract).

Feng, Z.Q., 2008. Volcanic rocks as prolific gas reservoir: a case study from the Qingshen gas field in the Songliao Basin, NE China. Mar. Pet. Geol. 25 (4–5), 416–432.

Filho, A.T., Mizusaki, A.M.P., Antonioli, L., 2008. Magmatism and petroleum exploration in the Brazilian Paleozoic basins. Mar. Pet. Geol. 25 (2), 143–151.

Fisher, R.V., Schmincke, H.U., 1984. Pyroclastic Rocks. Springer Berlin Heidelberg, Berlin, pp. 1–472.

Gaonac'h, H., Lovejoy, S., Schertzer, D., 2005. Scaling vesicle distributions and volcanic eruptions. Bull. Volcano 67, 350–357.

Ge, R.F., Zhang, Q.L., Wang, L.S., Chen, J., Xie, G.A., Wang, X.Y., 2012. Late Mesozoic rift evolution and crustal extension in the central Songliao Basin, northeastern China: constraints from cross-section restoration and implications for lithospheric thinning. Int. Geol. Rev. 54 (2), 183–207.

Gu, L.X., Ren, Z.W., Wu, C.Z., Zhao, M., Qiu, J., 2002. Hydrocarbon reservoirs in a trachyte porphyry intrusion in the Eastern depression of the Liaohe basin, northeast China. AAPG (Am. Assoc. Pet. Geol.) Bull. 86 (10), 1821–1832.

Hou, L.H., Zou, C.N., Liu, L., Wen, B.H., Wu, X.Z., Wei, Y.Z., Mao, Z.G., 2012. Geologic essential elements for hydrocarbon accumulation within Carboniferous volcanic weathered crusts in Northern Xinjiang, China. Acta Pet. Sin. 33 (4), 533–540 (in Chinese with English abstract).

Huang, S.J., Huang, K.K., Feng, W.L., Tong, H.P., Liu, L.H., 2009. Mass exchanges among Feldspar, kaolinite and illite and their influences on secondary porosity formation in clastic diagenesis ——a case study on the Upper Paleozoic, Ordos Basin and Xujiahe Formation ,Western Sichuan Depression. Geochimica 38 (5), 498–506 (in Chinese with English abstract).

Huang, S.J., Wu, W.H., Liu, J., Sheng, L.C., Huang, C.G., 2003. Generation of secondary porosity by meteoric water during time of subaerial exposure: an example from Yanchang formation sandstone of Triassic of Ordos basin. Earth Sci. J. China Univ. Geosci. 28 (4), 419–424 (in Chinese with English abstract).

Huang, Z.L., Liu, B., Luo, Q.S., Wu, H.Z., Ma, J., Chen, X., Chen, J.Q., 2012. Main controlling factors and models of Carboniferous volcanic hydrocarbon accumulation in the Malang Sag, Santang basin. Acta Geol. Sin. 86 (8), 1210–1216 (in Chinese with English abstract).

Inoue, A., Meunier, A., Patrier-Mas, P., Rigault, C., Beafort, D., Vieillard, P., 2009. Application of chemical geothermometry to low-temperature trioctahedral chlorites. Clay Clay Miner. 57 (3), 371–382.

Jerram, D.A., Single, R.T., Richard, W.H., Catherine, E.N., 2009. Understanding the offshore flood basalt sequence using onshore volcanic facies analogues: an example from the Faroe–Shetland basin. Geol. Mag. 146 (3), 353–367.

Jia, C.Z., Zhao, W.Z., Zou, C.N., Feng, Z.Q., Yuan, X.J., Chi, Y.L., Tao, S.Z., Xue, S.H.,

2007. Geological theory and exploration technology for lithostratigraphic hydrocarbon reservoirs. Pet. Explor. Dev. 34 (3), 257–272 (in Chinese with English abstract).
Jiang, F., Cheng, R.H., Ruan, B.T., Lin, B., Xu, Z.J., Li, Z.C., 2017. Formation mechanism of volcanic reservoirs within a volcanostratigraphy framework: the case of the Wangfu fault depression in the Songliao Basin, China. Mar. Pet. Geol. 84, 160–178.
Jin, Q., Xu, L., Wan, C.L., 2007. Interactions between basalts and oil source rocks in rift basins: CO_2 generation. Chin. J. Geochem. 26, 58–65.
Jones, S.F., Wielens, H., Williamson, M.C., Zentilli, M., 2007. Impact of magmatism on petroleum systems in the Sverdrup Basin, Canadian Arctic Islands, Nunavut: a numerical modelling study. J. Pet. Geol. 30 (3), 237–256.
Kawamoto, T., 2001. Distribution and alteration of the volcanic reservoir in the Minami-Nagaoka gas field. J. Jpn. Ass. Pet. Technol. 66, 46–55.
Kirsimae, K., Suuroja, S., Kirsi, J., Karki, A., Polikarpusi, M., Puura, V., Suuroja, K., 2002. Hornblende alteration and fluid inclusions in Kardla impact crater, Estonia: evidence for impact-induced hydrothermal activity. Meteorit. Planet. Sci. 37, 449–457.
Klug, C., Cashman, K.V., 1996. Permeability development in vesiculating magmas: implications for fragmentation. Bull. Volcanol. 58, 87–100.
Kontorovich, A.E., Khomenko, A.V., 2001. Theoretical foundations of predicting the petroleum potential of sedimentary basins with intense manifestation of trap magmatism. Geol. Geofiz. 42 (11–12), 1764–1773.
Kus, J., Cramer, B., Kocke, F., 2005. Effects of a Cretaceous structural inversion and a postulated high heat flow event on petroleum system of the western Lower Saxony Basin and the charge history of the Apeldorn gas field. Netherlands J. Geosci.-Geol. En Mijnb. 84 (1), 3–24.
Laubach, S.E., Ward, M.E., 2006. Diagenesis in porosity evolution of opening-mode fractures, middle Triassic to lower Jurassic La Boca formation, NE Mexico. Tectonophysics 419, 75–97.
Li, J.Z., Ding, X.Y., Zhang, J.J., Yao, D.M., Wang, Z.J., 1988. Synthesis of rhodonite its solubility in various acids. J. Beijing Univ. Iron Stell Technol. 10 (1), 113–118 (in Chinese with English abstract).
Liu, J.Q., FC, M., Cui, Y., Zhang, Y.T., 2010. Discussion on the formation mechanism of volcanic oil and gas reservoirs. Acta Petrol. Sin. 26 (1), 1–13 (in Chinese with English abstract).
Liu, L.Y., Chen, G., Liu, Y.Q., Di, S.X., Xue, X.X., 1998. Analysis on influencing factors of solution-type secondary pore- evolution in clastic reservoirs. Acta Sedimentol. Sin. 16 (2), 97–101 (in Chinese with English abstract).
Lovejoy, S., Gaonac'h, H., Schertzer, D., 2004. Bubble distributions, and dynamics: the expansion-coalescence equation. J. Geophys. Res. 109 (B11), 202–244.
Luo, J.L., Hou, L.H., Jiang, Y.Q., 2012. Chronology and tectonic settings of igneous rocks and origin of volcanic reservoirs in Ludong area, eastern Junggar Basin. Acta Pet. Sin. 33 (3), 351–360 (in Chinese with English abstract).
Luo, J.L., Shao, H.M., Yang, Y.F., Li, S., Lou, C.Y., 2013. Temporal and spatial evolution of buried-hydrocarbon filling-diagenetic process of deep volcanic reservoir in Songliao Basin. Earth Sci. Front. 20 (5), 175–187 (in Chinese with English abstract).
Luo, J.L., Zhang, C.L., Qu, Z., 1999. Volcanic reservoir rocks: a case study of the cretaceous Fenghuadian suite, Huanghua Basin, Eastern China. J. Pet. Geol. 22, 397–415.
Mao, Z.G., Zhu, R.K., Luo, J.L., Wang, J.H., Du, Z.H., Su, L., Zhang, S.M., 2015. Reservoir characteristics, formation mechanisms and petroleum exploration potential of volcanic rocks in China. Pet. Sci. 12 (1), 54–66.
Mc Phie, J., Doyle, M., Allen, R., 1993. Volcanic Textures. A Guide to the Interpretation of Textures in Volcanic Rocks. University of Tasmania, Tasmania, pp. 196.
Neuendorf, K.K.E., Mehl, J.P., Jackson, J.A., 2011. Glossary of Geology (Fourth Edition). American Geosciences Institute Alexandria, Virginia, pp. 1–779.
Noguera, C., Fritz, B., Clément, A., 2011. Simulation of the nucleation and growth of clay minerals coupled with cation exchange. Geochem. Cosmochim. Acta 75, 3402–3418.
Olson, J.E., Laubach, S.E., Lander, R.H., 2009. Natural fracture characterization in tight gas sandstones: integrating mechanics and diagenesis. AAPG (Am. Assoc. Pet. Geol.) Bull. 93 (11), 1535–1549.
Othman, R., Colin, R., Ward, 2002. Thermal maturation pattern in the southern Bowen, northern gunnedah and Surat basins, northern new South Wales, Australia. Int. J. Coal Geol. 51 (3), 145–167.
Polyansky, O.P., Reverdatto, V.V., Khomenko, A.V., Kuznetsova, E.N., 2003. Modeling of fluid flow and heat transfer induced by basaltic near-surface magmatism in the Lena-Tunguska petroleum basin (Eastern Siberia, Russia). J. Geochem. Explor. 78–79, 687–692.
Ren, Z.L., Xiao, D.M., Chi, Y.L., 2001. Restoration of the palaeogeotherm in Songliao basin. Petroleum Geol. Oilf. Dev. Daqing 20 (1), 13–15 in Chinese with English abstract.
Rowe, M.C., Ellis, B.S., Lindeberg, A., 2012. Quantifying crystallization and devitrification of rhyolites by means of X-ray diffraction and electron microprobe analysis. Am. Mineral. 97, 1685–1699.
Schutter, S.R., 2003. Occurrences of hydrocarbons in and around igneous rocks. Geol. Soc. Lon. Spec. Publ. 214, 35–68.
Sruoga, P., Rubinstein, N., 2007. Processes controlling porosity and permeability in volcanic reservoirs from the Austral and Neuquén basins, Argentina. AAPG (Am. Assoc. Pet. Geol.) Bull. 91 (1), 115–129.
Sruoga, P., Rubinstein, N., Hinterwimmer, G., 2004. Porosity and permeability in volcanic rocks: a case study on the Serie Tob|¤fera, South Patagonia, Argentina. J. Volcanol. Geotherm. Res. 132, 31–43.
Stagpoole, V., Funnell, R., 2001. Arc magmatism and hydrocarbon generation in the northern Taranaki basin, New Zealand. Pet. Geosci. 7, 255–267.
Tao, S.Z., Li, C.W., Ma, W.J., Liu, D.L., Mi, J.K., Pang, Z.L., 2017. Geochemical analysis and origin of gas in volcanic reservoirs in the Songliao Basin. Energy Explor. Exploit. 35 (3), 295–314.
Tang, H.F., Bai, B., Bian, W.H., Wang, L.Y., Sun, H.B., 2012a. Quantitative models of strata texture within volcanic edifices of Yingcheng Formation in the Songliao Basin, NE China. Acta Pet. Sin. 33 (4), 541–550 (in Chinese with English abstract).
Tang, H.F., Cryton, P., Gao, Y.F., Huang, Y.L., Bian, W.H., 2015. Types and characeristics of volcanostratigraphy boundaries and their oil-gas reservoir significance. Acta Geol. Sin. 89 (1), 163–174.
Tang, H.F., Hu, J., Li, J.H., Chen, M.F., Gao, Y.F., 2018. Geological significances of typical seismic facies of volcanic rocks of the rifted period in Songliao Basin, NE China. Oil Geophys. Prospect. 53 (5), 1705–1804.
Tang, H.F., Kong, T., Liu, X., Yang, D., Huo, H.Y., Huang, Y.L., 2016b. Characteristics and formation mechanism of high quality reservoir of volcaniclastic sedimentary rocks of early cretaceous in Songliao Basin. Acta Pet. Sin. 37 (5), 631–643 (in Chinese with English abstract).
Tang, H.F., Li, R.L., Wu, Y.H., Feng, X.H., Wang, L.Y., 2011. Textural characteristics of volcanic strata and its constraint to impedance inversion. Chin. J. Geophys. 54 (2), 620–627 (in Chinese with English abstract).
Tang, H.F., Pang, Y.M., Bian, W.H., 2008. Quantitative analysis on reservoirs in volcanic edifice of early cretaceous Yingcheng Formation in Songliao Basin. Acta Pet. Sin. 29 (6), 841–845 (in Chinese with English abstract).
Tang, H.F., Sun, H.B., Gao, Y.F., Yi, J., Yao, R.S., 2013. Types and characteristics of volcanostratigraphy boundary and its signification of reservoirs. J. Jilin Univ. (Earth Sci. Ed.) 43 (5), 1320–1329 (in Chinese with English abstract).
Tang, H.F., Xu, Z.S., Wu, Y.H., Wu, Y.X., 2010. Characteristics and controlling factors of volcanic reservoir flow units of Yingcheng Formation in the Songliao Basin. Acta Petrol. Sin. 26 (1), 55–62 (in Chinese with English abstract).
Tang, H.F., Yang, D., Shao, M.L., Wang, P.J., Sun, W.T., Huang, Y.L., 2016a. The constraints of the environment of deposition of volcanostratigraphy emplacement to the distributive pattern of reservoirs: a case study of the rhyolitic volcanostratigraphy in the 2nd member of Jurassic Huosjiling formation in Wangfu fault depression, Songliao Basin. Pet. Explor. Dev. 43 (4), 626–633.
Tang, H.F., Zhao, X.Y., Shao, M.L., Sun, X.D., Zhang, Y., Phiri, C., 2017a. Reservoir origin and characterization of gas pools in intrusive rocks of the Yingcheng Formation, Songliao Basin, NE China. Mar. Pet. Geol. 84, 148–159.
Tang, H.F., Kong, T., Wu, C.Z., Wang, P.J., Peng, X., Gao, Y.F., 2017b. Filling pattern of volcanostratigraphy of cenozoic volcanic rocks in the Changbaishan Area and possible future eruptions. Acta Geol. Sin.-Engl. Ed. 91 (5), 1717–1732.
Tang, L.J., Huang, T.Z., Qiu, H.J., Cui, Z.H., Wan, G.M., Jin, X.M., Yang, S.J., 2012c. The tectonic characteristics and hydrocarbon accumulation of late Hercynian volcanic rocks in the Tahe area, Tarim Basin. Acta Geol. Sin. 86 (8), 1188–1197 (in Chinese with English abstract).
Uliana, M.A., Biddle, K.T., Cerdáan, J., 1989. Mesozoic extension and formation of Argentina sedimentary basin: extensional tectonics and stratigraphy of the North Atlantic margin. AAPG Mem. 46, 599–613.
Volk, H., Horsfield, B., Mann, Ulrich, Suchý, V., 2002. Variability of petroleum inclusions in vein, fossil and vugcements—a geochemical study in the Barrandian Basin (Lower Palaeozoic, Czech Republic). Org. Geochem. 33, 1319–1341.
Wang, J.H., Jin, J.Q., Zhu, R.K., 2011. Characters and distribution patterns of effective reservoirs in the Carboniferous volcanic weathering crust in Northern Xinjiang. Acta Pet. Sin. 32 (5), 757–766 (in Chinese with English abstract).
Wang, J.W., Bao, Z.D., Chen, M.J., Sun, F.J., Liu, R.E., Zhao, M.F., Sun, Q.Y., 2005. Differentiation of sandstone tuff filling and its effect on poro Sity—an example from the paleozoic in Northwestern Ordos. Chin. J. Geol. 40 (3), 429–438 (in Chinese with English abstract).
Wang, P.J., Chen, S.M., 2015. Cretaceous volcanic reservoirs and their exploration in the Songliao Basin, northeast China. AAPG (Am. Assoc. Pet. Geol.) Bull. 99 (3), 499–523.
Wang, P.J., Du, X.D., Wang, J., Wang, D.P., 1995. Chronostratigraphy and stratigraphic classification of the Cretaceous of Songliao basin. Acta Geol. Sin. 69 (4), 372–381 (in Chinese with English abstract).
Wang, P.J., Liu, W.Z., Wang, S.X., Song, W.H., 2002. 40Ar/39Ar and K/Ar dating on the volcanic rocks in the Songliao Basin, NE China: constraints on stratigraphy and basin dynamics. Int. J. Earth Sci. 91, 331–340.
Wang, P.J., Mattern, F., Didenko, N.A., Zhu, D.F., Singer, B., Sun, X.M., 2016. Tectonics and cycle system of the Cretaceous Songliao Basin: an inverted active continental margin basin. Earth Sci. Rev. 159, 82–102.
Wang, P.J., Wu, H.Y., Pang, Y.M., Men, G.T., Ren, Y.G., Liu, W.Z., Bian, W.H., 2006. Volcanic facies of the Songliao Basin: sequence, model and the quantitative relationship with porosity & permeability of the volcanic reservoir. J. Jilin Univ.: Earth Sci. Ed. 36 (5), 805–812 (in Chinese with English abstract).
Wang, Y.Z., Cao, Y.C., Xi, K.L., 2013. New View on the concept of secondary pore developing zones and its significance of petroleum geology. J. Jilin Univ. (Earth Sci. Ed.) 43 (3), 659–679 (in Chinese with English abstract).
Watton, T.J., Wright, K.A., Jerram, D.A., Brown, R.J., 2014. The petrophysical and petrographical properties of hyaloclastite deposits: implications for petroleum exploration. AAPG (Am. Assoc. Pet. Geol.) Bull. 98 (3), 449–463.
Wu, C.Z., Gu, L.X., Zhang, Z.Z., Ren, Z.W., Chen, Z.Y., Li, W.Q., 2006. Formation mechanisms of hydrocarbon reservoirs associated with volcanic and subvolcanic intrusive rocks: examples in Mesozoic–Cenozoic basins of eastern China. AAPG (Am. Assoc. Pet. Geol.) Bull. 90 (1), 137–147.
Yang, C., Hou, L., et al., 2017. Controlling factors of volcanic hydrocarbon reservoirs in Bohai Bay Basin, China. J. Nat. Gas Geosci. 2, 219–228.
Yang, B.J., Liu, W.S., Wang, X.C., Li, Q.X., Wang, J.M., Zhao, X.P., Li, R.L., 2005. Geophysical characteristics of Daxinganling gravitational gradient zone in the East China and its geodynamic mechanism. Chin. J. Geophys. 48 (1), 86–97 (in Chinese with English abstract).
Yang, X.N., Chen, H.D., Shou, J.F., Zhang, H.L., 2004. Mechanism of the formation of secondary porosity in clastic rock. J. Daqing Pet. Inst. 28 (1), 4–6 (in Chinese with

English abstract).
Yi, J., Tang, H.F., Wang, P.J., Gao, Y.F., Zhao, R.L., 2016. Types, characteristics and reservoir significance of basic lava flow units. J. Cent. South Univ. 47 (1), 149–158 (in Chinese with English abstract).
Yi, J., Wang, P.J., Li, R.L., Zhao, R.L., Chen, C.Y., Sun, Y., 2014. Seismic volcanostratigraphy of the Songliao Basin, early cretaceous: typical interpretation pattern. J. Jilin Univ.: Earth Sci. Ed. 44 (3), 715–729.
Yi, J., Wang, P.J., Tang, H.F., Zhao, R.L., Yao, R.S., Hao, G.L., Gao, Y.F., 2015. Geological property, Geological connotation and reservoir significance of volcanostratigraphy boundary: a case study of the Mesozoic & Cenozoic volcanic rocks in northeastern China. Acta Pet. Sin. 36 (3), 324–336 (in Chinese with English abstract).
Zhang, G.F., Yan, D.C., Zhu, Y.Y., Feng, Q.M., Wang, W.Q., 2011. Influence of pH on adsorption of sodium oleate on surface of ilmenite and titanaugite. J. Cent. South Univ. 42 (10), 2898–2904 (in Chinese with English abstract).
Zhang, J., 2013. Reservoir Forming Conditions of Deep Gas in Wangfu Faulted depression [D]. Northeast Petroleum University (in Chinese with English abstract).
Zhang, L.Y., Ji, Y.L., Liu, L., Zhang, G., Zhao, L., Mu, H.Y., 2012. Origin of anomalously high porosity in pyroclastic reservoirs: a case study on the northern region of the east sub-sag in Nanbeier sag. Acta Pet. Sin. 33 (5), 814–821 (in Chinese with English abstract).
Zheng, J.M., Ying, F.X., 1997. Reservoir characteristic and diagenetic model of sandstone intercalated in coal-bearing strata. Acta Pet. Sin. 18 (4), 19–24 (in Chinese with English abstract).
Zheng, H., Sun, X.M., Zhu, D.F., Tian, J.X., Wang, P.J., Zhang, X.Q., 2018. Characteristics and factors controlling reservoir space in the Cretaceous volcanic rocks of the Hailar Basin, NE China. Mar. Pet. Geol. 91, 749–763.
Zhong, D.K., Zhu, X.M., Zhang, Z.H., Zhang, Q., 2003. Origin of secondary porosity of paleogene sandstone in the Dongying sag. Pet. Explor. Dev. 30 (6), 51–53 (in Chinese with English abstract).
Zou, C.N., Hou, L.H., Tao, S.Z., Yuan, R.K., Zhang, X.X., Li, F.H., Pang, Z.L., 2011. Hydrocarbon accumulation mechanism and structure of large-scale volcanic weathering crust of the Carboniferous in Northern Xinjiang, China. Sci. China Earth Sci. 41 (11), 1613–1626 (in Chinese with English abstract).